RECOMBINANT PHAGE ENDOLYSIN

AS ANTIBIOFILM AGENT

AGAINST *STAPHYLOCOCCUS AUREUS*

AND *PSEUDOMONAS AERUGINOSA*

YEONG ZI HUI

BACHELOR OF SCIENCE (HONS)

BIOMEDICAL SCIENCE

FACULTY OF SCIENCE

UNIVERSITI TUNKU ABDUL RAHMAN

MAY 2024

RECOMBINANT PHAGE ENDOLYSIN AS ANTIBIOFILM AGENT AGAINST *STAPHYLOCOCCUS AUREUS* AND *PSEUDOMONAS AERUGINOSA*

By

YEONG ZI HUI

A project report submitted to the Department of Allied Health Sciences

Faculty of Science

Universiti Tunku Abdul Rahman

in partial of fulfillment of the requirements for the degree of

Bachelor of Science (Hons) Biomedical Science

May 2024

ABSTRACT

RECOMBINANT PHAGE ENDOLYSIN AS ANTIBIOFILM AGENT AGAINST *STAPHYLOCOCCUS AUREUS* AND *PSEUDOMONAS AERUGINOSA*

YEONG ZI HUI

The rising number of antimicrobial-resistant (AMR) bacteria is a major global threat. The ESKAPE pathogens, *Staphylococcus aureus* and *Pseudomonas aeruginosa* commonly cause biofilm-associated infections. Biofilm formation further enhances antibiotic resistance, compromising conventional therapies. This triggers an urgent search for alternative therapies to combat biofilms, such as phage endolysin. The ability of phage endolysins to cut as anti-bacterial agents was reported in previous studies. Thus, different recombinant endolysins have been produced and investigated for their ability to control pathogens. Likewise, in this study, the endolysin gene, which originated from a novel phage (*Escherichia* phage KW1E_UTAR), has been cloned and expressed as recombinant endolysin. The recombinant endolysin was shown in a previous study to exhibit an antibacterial effect against *S. aureus* and *P. aeruginosa*. However, its antibiofilm activity has not been investigated. Therefore, in this study, both the inhibitory and eradication effect of this recombinant endolysin was determined. Firstly, the *S. aureus* and *P. aeruginosa* biofilm formation was optimized. Results showed that both bacteria were strong biofilm producers when cultivated in TSB supplemented with 1.0% (v/v) glucose with an initial

and incubated at 37℃. bacterial titer of 10^8 CFU/mL and incubated at 37℃. Subsequently, the antibiofilm effects of the recombinant endolysins were investigated. The results showed that the minimum 50% biofilm inhibition concentrations ($MBIC_{50}$) against *S. aureus* and *P. aeruginosa* were 1.95 – 7.81 µg/mL and 0.98 µg/mL, respectively. However, $MBIC_{90}$ for both bacteria was not achieved in this study. On the other hand, the minimum 50% biofilm eradication concentrations ($MBEC_{50}$) against *S. aureus* and *P. aeruginosa* were 15.63 – 31.25 µg/mL and 1.95 µg/mL, respectively. Meanwhile, only $MBEC_{90}$ against *P. aeruginosa* was determined at 3.91 – 15.63 µg/mL. Therefore, the present study suggests that the recombinant endolysin can be further explored as an antibiofilm agent clinically isolated *S. aureus* and *P. aeruginosa*.

ACKNOWLEDGEMENTS

DECLARATION

I hereby declare that this final year project is based on my original work except for quotations and citations which have been duly acknowledged. I also declare that it has not been previously or concurrently submitted for any other degree at UTAR or other institutions.

(YEONG ZI HUI)

APPROVAL SHEET

The final year project report entitled "**RECOMBINANT PHAGE ENDOLYSIN AS ANTIBIOFILM AGENT AGAINST *STAPHYLOCOCCUS AUREUS* AND *PSEUDOMONAS AERUGINOSA*"** was prepared by YEONG ZI HUI and submitted as partial fulfilment of the requirements for the degree of Bachelor of Science (Hons) Biomedical Science at Universiti Tunku Abdul Rahman.

Approved by:

_____

(Dr. MICHELLE NG YEEN TAN)   Date: 25 April 2024

Supervisor

Department of Allied Health Sciences

Faculty of Science

Universiti Tunku Abdul Rahman

TABLE OF CONTENTS

LIST OF TABLES

LIST OF FIGURES

LIST OF ABBREVATIONS

AAC	Aminoglycoside acetyltransferase
ABC	ATP-binding cassette
A. baumannii	*Acinetobacter baumannii*
AIs	Autoinducers
ALT	Antibiotic lock therapy
AMP	Antimicrobial peptide
AMR	Antimicrobial resistance
ANT	Aminoglycoside nucleotidyltransferase
APH	Aminoglycoside phosphotransferase
APS	Ammonium persulfate
ATCC	American type culture collection
BSA	Bovine serum albumin
CBD	Cell wall-binding domain
c-di-GMP	Cyclic dimeric guanosine monophosphate
CHAP	Cysteine-histidine dependent amino-hydrolase/peptidase
CST	Colistin
CV	Crystal violet
CVC	Central venous catheters
D-Ala-D-Ala	D-alanyl-D-alanine
D-Ala-D-Lac	D-alanyl-D-lactate
EAD	Enzymatically active domain
ECM	Extracellular matrix

eDNA	Extracellular DNA
EDTA	Ethylenediaminetetraacetic acid
E. coli	*Escherichia coli*
E. faecalis	*Enterococcus faecalis*
EPS	Extracellular polymeric substances
HAI	Healthcare-associated infections
H. pylori	*Helicobacter pylori*
IPTG	Isopropyl B-D-1-Thiogalactopyranoside
K. pneumoniae	*Klebsiella pneumoniae*
LB	Luria Bertani
L. monocytogenes	*Listeria monocytogenes*
MATE	Multidrug and toxic compound extrusion
MBIC	Minimum biofilm inhibitory concentration
MBEC	Minimum biofilm eradication concentration
MDR	Multidrug resistance
MFS	Major facilitator superfamily
MgO	Magnesium oxide
MIC	Minimum inhibitory concentration
MRSA	Methicillin-resistant *S. aureus*
MWCO	Molecular weight cut-off
NAG	N-acetyglucosamines
NAM	N-acetylmuramic acids
nc	Negative control
OD	Optical density
ODc	Cut-off value

ODnc	OD of the negative control
P. aeruginosa	*Pseudomonas aeruginosa*
PBP	Penicillin-binding proteins
PBS	Phosphate buffered saline
PDT	Photodynamic therapy
PGH	Peptidoglycan hydrolase
Phage	bacteriophage
P. mirabilis	*Proteus mirabilis*
RND	Resistance-nodulation-cell division
SAB	Sample loading buffer
S. aureus	*Staphylococcus aureus*
SAR	Signal-arrest-release
SDnc	standard deviation
SDS	Sodium dodecyl sulfate
SDS-PAGE	Sodium dodecyl sulfate-polyacrylamide gel electrophoresis
S. epidermidis	*Staphylococcus epidermidis*
SMR	Small multidrug resistance
SrtA	Sortase A
S. viridans	*Streptococcus viridans*
TEMED	Tetramethylethylenediamine
TGC	Tigecycline
TSB	Tryptic soy broth
VRSA	Vancomycin-resistant *S. aureus*
XDR	Extensively drug-resistant

CHAPTER 1

INTRODUCTION

The emergence of antimicrobial resistance (AMR) or multidrug resistance (MDR), in which drugs are no longer effective in killing microbes, has been one of the major threats in the global medical setting (World Health Organization [WHO], 2023). Normally, bacterial infections can be treated with antibiotics. However, overusage of antibiotics, such as unnecessary consumption of antibiotics or consumption of wrong doses of antibiotics, has led to the emergence of antibiotic-resistant bacteria (Villines, 2023; Lu, et al., 2021, Pachori, Gothalwal and Gandhi, 2019). Bacteria that were used to be susceptible to certain antibiotics have now developed resistance to those antibiotics, thus, treating MDR bacterial infections has become more challenging (Pachori, Gothalwal and Gandhi, 2019).

On top of that, according to an analysis conducted by Murray in 2019, 1.27 million global deaths were attributed to AMR (Murray, 2022). *Staphylococcus aureus* and *Pseudomonas aeruginosa* are the two of the six most virulent bacteria which responsible for 250,000 deaths attributed to AMR. In addition, these two bacteria are classified as ESKAPE pathogens. ESKAPE is an acronym for the six most virulent and AMR bacteria which include – *Enterococcus faecium*, *Staphylococcus aureus*, *Klebsiella pneumoniae*, *Acinetobacter baumannii*, *Pseudomonas aeruginosa* and *Enterobacter* species (Santajit and Indrawattana, 2016). The biofilm formation ability of *Staphylococcus aureus* and *Pseudomonas aeruginosa* is one of the factors that contributes to

AMR and results in the increased risk of chronic infectious diseases (Fursov, et al., 2020; Ryan, 2022). Therefore, it is vital to develop alternative treatments to combat the biofilms formed by AMR bacteria.

Currently, the alternative agents and therapies available to treat biofilm formation are antimicrobial peptide (AMP), nanoparticles, phytochemicals, photodynamic therapy (PDT) and phage therapy (Yasir, Willcox and Dutta, 2018; Sharma, Misba and Khan, 2019; Mishra, et al., 2020; Liu, et al., 2022; Swidan, et al., 2022). Phage therapy uses bacteriophage, a virus that specifically kills bacteria, to treat bacterial infections (Barron, 2022). Bacteriophages are widely found in the environments as well as in human bodies, hence, they are easily accessible (Liu, et al., 2023). An enzyme produced by the bacteriophage, known as endolysin which hydrolyzes the peptidoglycans of the bacterial cell wall, has become the interest in developing it as a novel antimicrobial agent (Schmelcher and Loessner, 2021).

At present, different recombinant endolysins have been developed and their antimicrobial activities have been evaluated (Liu, et al., 2023). Recombinant endolysins have a broader host range with a faster antimicrobial activity than their parental phages (Liu, et al., 2023). Most importantly, recombinant endolysins have very low side effects, toxicity and risk of resistance development as compared to conventional antibiotic therapy (Ellen, et al., 2021; Rahman, et al., 2021).

In this study, a recombinant endolysin from a novel bacteriophage isolated from a hot spring has been shown to be effective against Gram-positive *S. aureus* and Gram-negative *P. aeruginosa*. However, the antibiofilm activity of this recombinant endolysin is yet to be clarified.

1.1 Objectives of Study

Therefore, the objectives of the study were to:

1. Optimize the growth of *S. aureus* and *P. aeruginosa* biofilm.

2. Determine the minimum biofilm inhibitory concentration (MBIC) of the recombinant phage endolysin against *S. aureus* and *P. aeruginosa*.

3. Determine the minimum biofilm eradication concentration (MBEC) of the recombinant phage endolysin against *S. aureus* and *P. aeruginosa*.

CHAPTER 2

LITERATURE REVIEW

2.1 Antimicrobial resistance (AMR) bacteria

2.1.1 *Staphylococcus aureus*

Staphylococcus aureus is a spherical, facultative bacterium that appears in clusters and has a Gram-positive cell wall (Willey, Sandman and Wood, 2020; Taylor and Unakal, 2023). It often leads to healthcare-associated infections (HAI) that most commonly cause infective endocarditis, pneumonia, osteomyelitis, toxic shock syndrome, and abscesses (Olsen, et al., 2018; Ryan, 2022; Van Der Schoor, et al., 2023).

Staphylococcus aureus is the most virulent pathogen among more than 40 known species in its genus (Ryan, 2022). The multidrug-resistant (MDR) strains such as methicillin-resistant *S. aureus* (MRSA) and vancomycin-resistant *S. aureus* (VRSA) were developed as *S. aureus* evolved to adapt to harsh environments like antibiotics. The phenotypic and physiological changes have enhanced its pathogenicity and resistance towards the antimicrobial agents (Riedel, et al., 2019).

A study conducted in Malaysia found that MRSA has the highest infection rates among six MDR bacteria over three years and it demonstrated a positive correlation with the increased consumption of antibiotics, particularly extended-spectrum cephalosporin and fluoroquinolones (Tan, et al., 2022). Apart from that, the most frequently used antibiotics such as beta-lactams, glycopeptides,

and oxazolidinones, were no longer effective in treating *S. aureus* infections (Mlynarczyk-Bonikowska, et al., 2022).

2.1.2 *Pseudomonas aeruginosa*

Pseudomonas aeruginosa is a flagellated, rod-shaped bacterium with a Gram-negative cell wall (Ryan, 2022; Wilson and Pandey, 2023). Nosocomial infections caused by *P. aeruginosa*, which include otitis externa, pneumonia, cystic fibrosis, osteomyelitis, catheter-associated urinary tract infection, and ecthyma gangrenosum have become more prevalent and caused a mortality rate of up to 62% in specific patient population (Ríos, et al., 2018; Wilson and Pandey, 2023; Ryan, 2022; Ng, et al., 2023). In addition, the global prevalence of nosocomial infections revealed that *P. aeruginosa* is among the most prevalent microorganisms causing infections in the region of the Americas (Raoofi, et al., 2023).

Pseudomonas aeruginosa is classified as a highly antibiotic-resistant bacterium because it is not susceptible to many of the frequently used antibiotics such as erythromycin, clindamycin, linezolid, daptomycin, vancomycin, ampicillin, penicillinase-resistant penicillin and tetracycline (Ryan, 2022). Similar to *S. aureus*, *P. aeruginosa* also has a high adaptability and evolution rate, which developed resistance against numerous antibiotics (Ng, et al., 2023). As a result of this extensively drug-resistant (XDR) property, it has become more and more challenging in treating *P. aeruginosa* infections.

2.1.3 Antimicrobial Resistant Mechanisms

An extensive range of antibiotics is insensitive to *S. aureus* and *P. aeruginosa* as mentioned in Sections 2.1.1 and 2.1.2. The primary mechanisms of antimicrobial resistance can be categorized into drug uptake limitation, drug target sites modification, drug inactivation, and active drug efflux systems, as shown in Figure 2.1 (Reygaert, 2018; Phang, et al., 2019; Mlynarczyk-Bonikowska, et al., 2022).
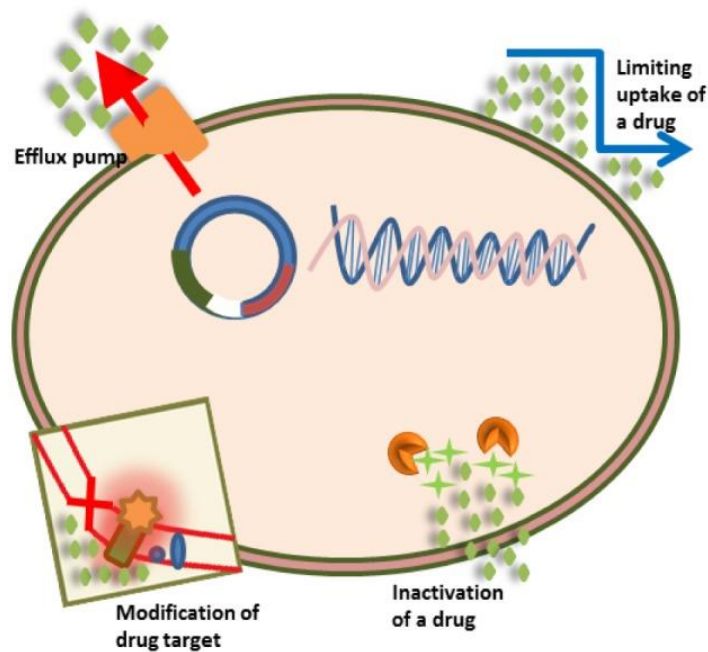
Figure 2.1: The general antimicrobial resistance mechanisms (Adapted from Reygaert, 2018).

The Gram-negative bacteria cell walls consist of outer membranes, which are less permeable to antibiotics, limiting the uptake of the drugs. The outer membranes comprise of phospholipid bilayer and lipopolysaccharides with porins embedded within them, as illustrated in Figure 2.2 (Tankeshwar, 2022).

6
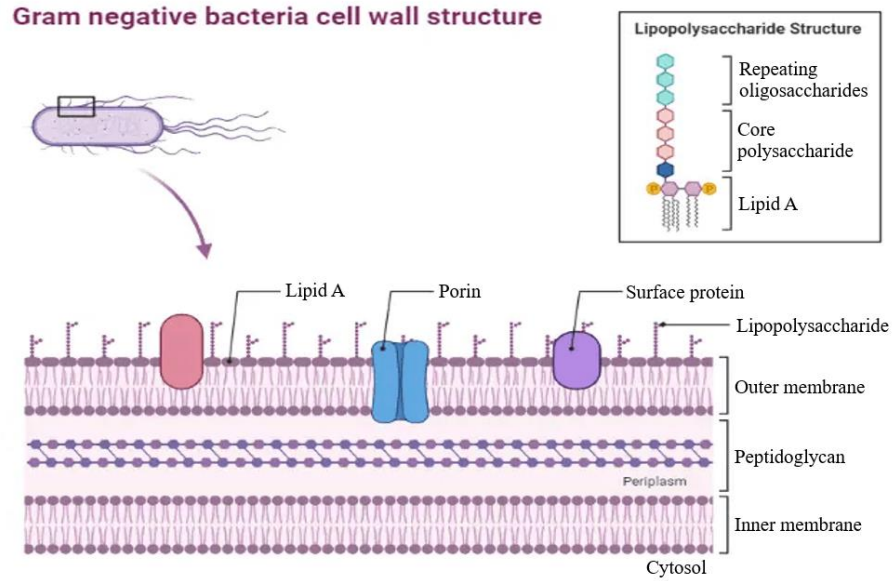
Figure 2.2: The structure of gram-negative bacterial cell wall (Adapted from Tankeshwar, 2022).

The primary non-specific porin that mostly present in *P. aeruginosa* outer membrane is called OprF (Phang, et al., 2019). Since most of the OprF channels are in closed conformation, this limits the uptake of antibiotics by the bacteria. On top of that, *P. aeruginosa* also lacks OprD, which is one of the specific porins and allows the uptake of antibiotics (Phang, et al., 2019). The absence of OprD leads to resistance towards carbapenems and β-lactams antibiotics (Phang, et al., 2019). In contrast, *S. aureus* has a gram-positive cell wall that lacks the outer membrane, but its thickened cell wall causes resistance to vancomycin due to the increased difficulty in penetrating the cell wall (Reygaert, 2018).

Moreover, altering the drug binding sites prevents the binding and action of the drug on its target sites. For instance, vancomycin targets the terminal D-alanyl-D-alanine (D-Ala-D-Ala), preventing the synthesis of peptidoglycan. The acquisition of *vanA* gene by *S. aureus* caused the D-alanyl-D-lactate (D-Ala-D-

Lac) formation instead of D-Ala-D-Ala which could not be bound by vancomycin (Cong, Yang and Rao, 2019). This allowed the complete synthesis of the peptidoglycan and survival of *S. aureus*. Thus, *S. aureus* that contains the vanA gene is classified as VRSA (Phukan, et al., 2016). Besides, DNA gyrase and topoisomerase are encoded by *gyrA* and *gyrB* genes and *parC* and *parE* genes, respectively, in *P. aeruginosa* (Phang, et al., 2019). DNA gyrase and topoisomerase IV are the targets for quinolones. Quinolones could not bind to the DNA gyrase and topoisomerase IV when the genes encoding for these proteins are mutated (Phang, et al., 2019). As a result, DNA gyrase and topoisomerase IV remain functional even in the presence of quinolones.

Furthermore, both bacteria produce enzymes that inactivate antibiotics by degrading the drug (Reygaert, 2018). β-lactamases are one of the enzymes produced by the bacteria to hydrolyze β-lactams antibiotics, which bind to penicillin-binding proteins (PBP) and prevent peptidoglycan synthesis (Reygaert, 2018). The inactivation of β-lactams causes no interference in the peptidoglycan synthesis. Antibiotics are also inactivated through acetylation, phosphorylation, or adenylation of the antibiotics. For instance, *P. aeruginosa* produces aminoglycoside phosphotransferase (APH), aminoglycoside acetyltransferase (AAC) and aminoglycoside nucleotidyltransferase (ANT) that modify the amino or hydroxyl groups of aminoglycosides, inactivating the aminoglycosides (Phang, et al., 2019). Whereas, *S. aureus* produces enzymes that acetylate chloramphenicol which could not inhibit *S. aureus* protein synthesis (Reygaert, 2018).

Staphylococcus aureus and *P. aeruginosa* also contain efflux pumps in their cell walls which actively expelling the toxic compounds including antibiotics out from the cells. The five predominant families of the efflux pumps are multidrug and toxic compound extrusion (MATE) family, major facilitator superfamily (MFS), small multidrug resistance (SMR) family, resistance-nodulation-cell division (RND) family, and ATP-binding cassette (ABC) family. In *S. aureus*, ABC, MFS, MATE or SMR families of multidrug efflux pumps are being identified (Dashtbani-Roozbehani and Brown, 2021). The NorA pump under MFS family leads to resistance against fluoroquinolones and chloramphenicol by *S. aureus* (Reygaert, 2018). On the other hand, the antibiotic resistance in *P. aeruginosa* is contributed by the RND family of efflux pumps which include MexAB-Opr, MMexCD-OprJ, MexEF-OprN, and MexXY-OprM.

2.2   Biofilm

Biofilms are often produced by *S. aureus* and *P. aeruginosa,* which further enhance the antibiotic resistance among the two bacteria. Biofilms are layers of microbial communities that adhere and grow on living or non-living surfaces through self-production of extracellular polymeric substances (EPS) (Assefa and Amare, 2022). The EPS produced by bacteria is made up of polysaccharides, proteins, extracellular DNA, and lipids (Di Martino, 2018; Pommerville, 2021). These components are essential to form a sticky extracellular matrix (ECM) that adheres the bacterial cells stably to the surface (Pommerville, 2021). Besides, the bacterial cells with biofilms are protected against hostile environments, which leads to resistance against the host defence system and antibacterial agents (Mirzaei, et al., 2020; Willey, Sandman and Wood, 2020). This is because

antibiotics are not able to penetrate through the ECM, which decreases their efficacy in eradicating the biofilm-embedded bacterial cells (Singh, et al., 2021; Mendhe, et al., 2023).

2.2.1 Biofilm Formation

Bacterial biofilm formation is a complex and multi-stage process which consists of five main stages – initial reversible attachment (1), irreversible attachment (2-3), maturation (4), and dispersion (5). Figure 2.3 depicts the phases of biofilm formation.
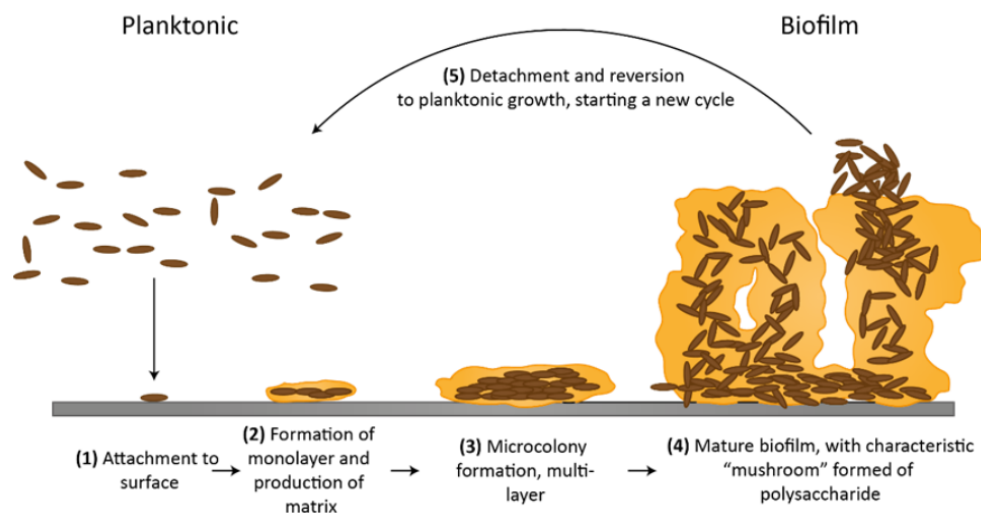
Figure 2.3: The phases involved in the biofilm formation (Adapted from Hollmann, Perkins and Walsh, 2018).

In the first stage, the synthesis of biofilms starts when the free-floating planktonic cells reversibly attached to a living or non-living surface with weak interactions such as van der Waals forces, hydrophobic interactions, and electrostatic forces (Muhammad, et al., 2020; Pommerville, 2021). If the environment permits, the bacterial cells proceed to form biofilm by forming a

monolayer of bacterial cells (stage two) with stronger adhesion to the surface using pili, flagella or a glycocalyx (Hollmann, Perkins and Walsh, 2018; Pommerville, 2021).

The bacterial cells then start to multiply and produce EPS (second stage) to further assist in a more stable attachment to one another and to the surface, forming microcolony (Pommerville, 2021; Rather, Gupta and Mandal, 2021). In this microcolony (third stage), the bacterial cells embedded in the matrix communicate with each other through a process known as quorum sensing. In quorum sensing, bacteria produce autoinducers (AIs), the chemical signalling molecules, to communicate and coordinate bacterial activities, including the activities of biofilm maturation (Willey, Sandman and Wood, 2020).

In the fourth stage, the maturation of biofilm takes place through cell division and EPS production regulated by the AIs. Moreover, the metabolic activities of the embedded bacterial cells differ as the biofilms grow, leading to biofilm heterogeneity, as shown in Figure 2.4 (Willey, Sandman and Wood, 2020). When the biofilm is fully matured, it resembles a pyramid-like living tissue structure consisting of water channels that function as a circulatory system to provide oxygen and nutrients, and eliminate waste from the cell community (Zhao, Sun and Liu, 2023; Pommerville, 2021).

In the last stage, the embedded bacterial cells detach from the mature biofilm and become planktonic cells that disperse into the environment (Muhammad, et al., 2020). This enables more planktonic cells to colonize new surfaces to start new cycles of biofilm formation (Willey, Sandman and Wood, 2020).
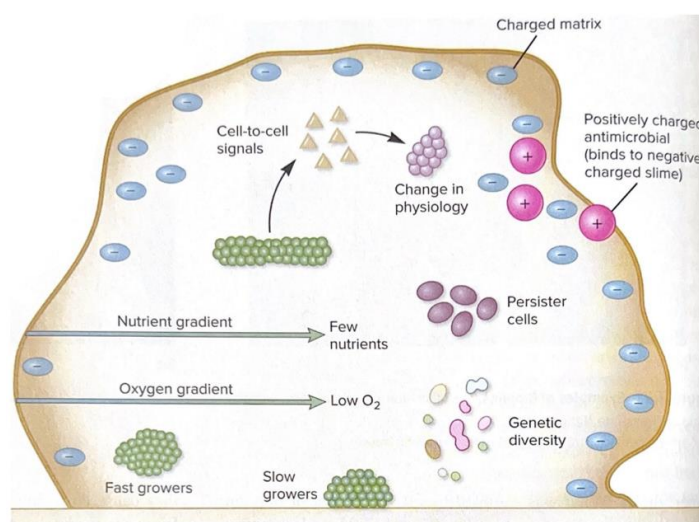
Figure 2.4: The biofilm heterogeneity (Adapted from Willey, Sandman and Wood, 2020).

2.2.2 Impacts of Biofilm Towards Human Health

Biofilm formation has severely impacted the healthcare industry. Recently, the demand for implantable medical devices has increased dramatically (Agrawal, et al., 2022). However, implantable medical devices, which include hip implants, contact lenses, intrauterine devices, urine catheters, prosthetic heart valves, and central venous catheters, are prone to biofilm formation (Shineh, et al., 2023). When the biofilms in the implants are exposed to biological fluids in the body, it leads to severe infections (Khatoon, et al., 2018; Shineh, et al., 2023). These implants could easily be contaminated with bacteria prior to implantation. Khatoon, et al, (2018) reported that *K. pneumoniae*, *E. coli*, *E. faecalis*, *P.*

aeruginosa, P. mirabilis, S. aureus, *S. epidermidis*, and *S. viridans* are the most common bacteria that form biofilms on medical devices.

Additionally, it is claimed that 40-50% of prosthetic heart valve infections, 50-70% of catheter biofilm infections, and 87% of bloodstream infections are caused by *S. aureus* and *S. epidermidis* (Khatoon, et al., 2018). Despite the antibiotic treatments, these bacteria can survive under the protective layers of biofilm, causing recalcitrant infections (Schulze, et al., 2021; Perry and Tan, 2023; Shineh, et al., 2023).

Chronic microbial infection is also one of the significant consequences of biofilm formation. Biofilms could be introduced into one's body when a medical implant or device contaminated with biofilms is implanted in the body (Schulze, et al., 2021). Besides, the pathogenic bacteria acquired from the healthcare system could also colonize in one's body and develop biofilms (Yang, et al., 2023). As aforementioned, biofilms are one of the evasion strategies where the bacteria could escape from the host immune system and resist antibiotic therapy (Shineh, et al., 2023). Although high dosages of antibiotics are used, biofilms still cannot be completely eradicated and cause persistent inflammation and recurrent infection (chronic infection) (Mendhe, et al., 2023; Shineh, et al., 2023; Yang, et al., 2023). In addition, over 80% of chronic infections were estimated to be caused by biofilms (Assefa and Amare, 2022).

Bacterial cells in the outermost layer start to detach from the surfaces of the implants or tissues in the later stage of biofilm growth. These clusters of cells then travel as septic emboli in the blood circulation which may obstruct the blood vessels, resulting in embolism (Preda and Săndulescu, 2019; Mirzaei, et al., 2020). Heart valves are also the common sites for biofilm formation (Su, et al., 2022). Thus, the emboli formed from the detached biofilm in the heart valves might travel in the pulmonary circulation and increase the risk of pulmonary embolism (Vyas and Goyal, 2022; Shineh, et al., 2023).

Delayed wound healing can also be caused by biofilm. A study conducted by Marano, et al. in 2015 found that *S. aureus* biofilm was able to prevent the migration of keratinocytes, while *S. aureus* and *P. aeruginosa* biofilms could prevent the proliferation of keratinocytes leading to delayed wound healing. Production of destructive enzymes and toxins by the persistent bacteria in the biofilm may interfere with the wound healing process (Marano, et al., 2015; Shineh, et al., 2023).

In a study, *P. aeruginosa* biofilm was reported to delay wound healing in a diabetic mouse model by two to four weeks compared to the control (Perry and Tan, 2023). In addition, rhamnolipids synthesized by *P. aeruginosa* would enhance the inflammation of the wound (Vestby, et al., 2020; Guzmán, Ortega and Rubio, 2024). Rhamnolipids are immunomodulators that can activate the immune cells, producing pro-inflammatory cytokines which induce inflammation (Guzmán, Ortega and Rubio, 2024). The enhanced inflammation would further damage the surrounding tissues and delay the wound healing.

2.2.3 Mechanism of Host Immune System Evasion and Antibiotic Resistance

The host immune system is important to protect one's body against any pathogens. Antibiotics are provided to assist the immune system to fight against the bacteria. However, some bacteria form biofilms that can evade the host immune system and antibiotics (Bamford, MacPhee and Stanley-Wall, 2023). The EPS produced by the biofilm bacterial cells forms the ECM that can prevent the immune cells and antibiotics from penetrating the biofilm (Phang et al., 2019). Hence, the immune cells and antibiotics could not penetrate into deeper layers of biofilms to eradicate the bacteria. Besides, the antibiotics could be trapped in the biofilm during the penetration of the biofilm, which is then degraded by the ECM enzymes (Pinto, et al., 2020).

The virulence factors of the biofilm bacteria enhance their survival against the immune system. Protease IV, an enzyme produced by *P. aeruginosa* causes degradation of complement proteins and antibodies (Cangui-Panchi, et al., 2023). Absence of complement proteins and antibodies prevents the opsonization of the bacteria and the activation of complementary cascades (Male, Peebles and Male, 2020). Besides, *S. aureus* produces leukocidins that lyse the leukocytes (Cangui-Panchi, et al., 2023).

Biofilm formation also leads to physiological changes in the bacterial cells, which are metabolically inactive with slower growth due to inadequate nutrients and oxygen (Willey, Sandman and Wood, 2020). Hence, the protein synthesis in these cells is greatly reduced. Antibiotics that prevent protein synthesis such

as tetracyclines, chloramphenicol, and aminoglycosides, would not be effective against the inner layer of biofilm bacterial cells (Reygaert, 2018).

Biofilm also promotes horizontal transfer of resistance genes (Reygaert, 2018; Pommerville, 2021). The EPS that is produced by the bacterial cells contains extracellular DNA (eDNA), which consists of antibiotic-resistance genes. These eDNA are taken up by the other bacterial cells embedded in the same EPS and develop resistance towards the particular antibiotics (Reygaert, 2018; Pommerville, 2021).

2.3   Treatments in Eradication of Biofilms

2.3.1   Conventional Treatments

Conventionally, bacterial infections are treated with antibiotics. However, the ability to form the ECM in the biofilm has resulted in less susceptibility of the bacteria to antibiotics (Pinto, et al., 2020). Consequently, high doses of antibiotics are administered to eliminate the biofilms (Pinto, et al., 2020; Perry and Tan, 2023). A study reported that antibiotics higher than the minimum inhibitory concentration (MIC) could not effectively remove biofilms formed by ESKAPE pathogens (Pletzer, Mansour and Hancock, 2018). Hence, the antibiotics MIC required to eradicate the biofilm is approximately over 1000-fold higher (Perry and Tan, 2023). Besides, central venous catheters (CVC) are also prone to biofilm formation. Thus, an antibiotic lock therapy (ALT) in which administration of high doses of antibiotics is used to treat CVC infections (Wolfmeier, et al., 2018).

The prolonged exposure to high concentrations of antibiotics is greatly detrimental to humans (Wolfmeier, et al., 2018). Humans' microbiota is one of the defense mechanisms in the body. The microbiota that lines the respiratory tracts, gastrointestinal tracts and genital tracts forms a protective barrier. In the intestine, this barrier prevents the colonization of pathogens on the intestine mucosal layer (Iacob, Iacob and Luminos, 2019). However, high doses of antibiotics severely damage the normal microbiota barrier. For instance, ceftriaxone, which was used to treat *S. aureus* biofilms, has significantly reduced the gut microbiota (Wang, et al. 2021). Then, the damaged microbiota triggered the activation of immune systems and the release of proinflammatory cytokines, which resulted in chronic hepatitis (Wang, et al. 2021). The gut microbiota is also important in food digestion (Fan and Pedersen, 2021). Reduced gut microbiota due to prolonged exposure to antibiotics greatly affects nutrient absorption.

At the same time, a combination of different classes of antibiotics are used to treat biofilm-associated infections (Wolfmeier, et al., 2018). The combination of colistin (CST) and tigecycline (TGC) showed an effective synergistic antibiofilm effect against the MDR *A. baumannii* (Sato, et al., 2021). The purpose of using antibiotic-combined therapy is to lower the antibiotic doses and decrease the risk of antibiotic resistance (Umemura, et al., 2022). However, low concentrations of the respective antibiotics in a combined therapy were still ineffective in eradicating the biofilms. At a lower level of CST and TGC, the expression of the biofilm-related genes was significantly increased, reducing the efficacy of the antibiotics (Sato, et al., 2021). Furthermore, drug-drug

interaction could also cause adverse drug reactions (Malik, Wani and Hashmi, 2020).

Moreover, if biofilms are formed on the implanted medical devices, removal of the devices would be the solution for biofilm infections (Roy, et al., 2018). However, this involves a surgical procedure to remove the implants and followed by antimicrobial therapy (Fakhro, et al., 2016). On top of surgical risks, there is a high possibility that dispersal of the biofilms occurs during the removal of the implants, causing recolonization of the bacteria in the body (Khatoon, et al., 2018). Thus, there is still a need for antibiotics administration to prevent the recolonization of the bacteria. As aforementioned, antibiotics would greatly affect the normal microbiota and increase the risk of secondary infections (Wang, et al. 2021; Patangia, et al., 2022).

The conventional treatment has profoundly used antibiotics. However, the toxicity of antibiotics and the development of resistance result in an urgent need to develop alternative treatments with minimal side effects against biofilm (Roy, et al., 2018).

2.3.2 Alternative Treatments

To date, there are several novel antibiofilm agents as well as alternative approaches being discovered and studied to inhibit and eradicate biofilm. Antimicrobial peptides are one of the antibiofilm agents that can disrupt the membrane potential of the biofilm-embedded cells, interrupt the signalling system among the bacterial cells, degrade the EPS, and downregulate the genes

that are involved in biofilm formation (Yasir, Willcox and Dutta, 2018). PAM-5, an antimicrobial peptide that has been modified, showed a rapid bacteriocidal activity against ATCC strains of *P. aeruginosa* and *E. coli* (Yuen, et al., 2023). Another study showed that bacteriocin BMP11 has a MIC value as low as 0.6 µg/mL against *L. monocytogenes* and is able to inhibit more than 80% of biofilm formation by *L. monocytogenes* at that MIC (Yi, et al., 2018).

Besides, phytochemicals, the secondary metabolites obtained from plant extracts, also show a promising anti-biofilm effect. Phytochemicals inhibit quorum sensing, produce reactive oxygen species, and disrupt the adhesion of the biofilm (Goncalves, et al., 2023). For instance, the analogs of topsentin prevent the adhesion of Gram-positive bacteria by inhibiting the transpeptidase sortase A (SrtA) (Parrino, et al., 2021). Hence, the topsentin analogs could effectively inhibit the biofilm formation.

Nanoparticles with the ability to interfere with glucan synthesis, cell adhesion, production of acid, and quorum sensing can act as an alternative treatment against biofilm (Sharma, Misba and Khan, 2019). Overproduction of reactive oxygen species by zinc oxide (ZnO) nanoparticles causes the lysis of Gram-positive bacteria (Lopez-Miranda, et al., 2023). Apart from oxidative stress, magnesium oxide (MgO) nanoparticles damage the cell membrane and interrupt the quorum-sensing process, killing and inhibiting the *S. epidermidis* biofilms (Nguyen, et al., 2018).

Moreover, biofilm can be effectively removed by lytic bacteriophages (Goodarzi, et al., 2022). This is proven by two lytic phages, vB_PaeM_SCUT-S1 (S1) and vB_PaeM_SCUT-S2 (S2), which could inhibit the formation of biofilms and eradicate the mature biofilms formed by *P. aeruginosa* at a low multiplicity of infection (Guo, et al., 2019). Bacteriophage produces depolymerases and lysins enzymes. The depolymerase can degrade the EPS, which enhances the penetration of bacteriophage to the inner part of the biofilm, while lysins, which are also known as endolysins, digest the peptidoglycan and facilitate the lysis the bacterial cells (Goodarzi, et al., 2022). It is known that the endolysins lead to the lysis of bacterial cells. Thus, the endolysins are further being studied as new antibiofilm agents.

2.4   Recombinant Phage Endolysin

Phage endolysin or phage-encoded peptidoglycan hydrolase (PGH) is an enzyme produced by bacteriophage (phage), a virus that infects and replicates in bacteria (Liu, et al., 2023). Figure 2.5 portrays the function of endolysins and holins in the lytic cycle of bacteriophage. Upon the infection of phage, phage exploits the host cell machinery for genome replication and protein production, including holins. Upon the release of phage progenies, holins would mediate the transport of endolysins across the cell wall from internally to access and cleave the peptidoglycan (Liu, et al., 2023). As a result, the cells are lysed, releasing the phage progenies.
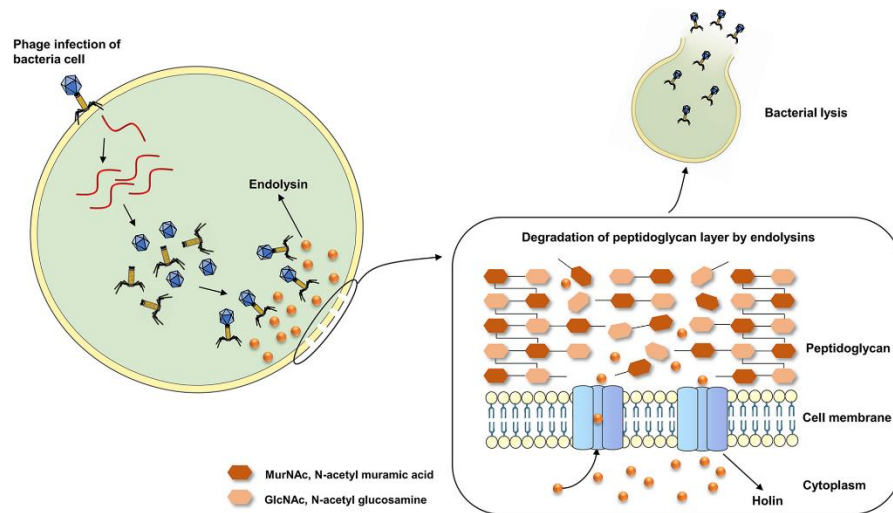
Figure 2.5: The function of endolysins and holins in a lytic cycle of bacteriophage. Pores in the cell membrane are formed by holins, increasing the permeability of the cell membrane towards endolysins. Then, the endolysins cleave the bonds between peptidoglycan components, MurNAc and GlcNAc, to release the new progenies through the lysis of the cell (Adapted from Liu, et al., 2023).

Endolysin could effectively lyse the bacterial cells, making it an ideal antibacterial agent. Thus, researchers started to develop recombinant endolysins which allowed the high yield and easy manipulation of the protein. The genes encoding endolysins are identified and cloned into bacterial plasmids, and induced to produce large amounts of recombinant endolysins (Zhang, et al., 2022). The recombinant endolysin is a small protein, which has a broader bacteriocidal specificity with rapid bacteriocidal activity and a lower risk of resistance (Zhang, et al., 2022). These properties of recombinant endolysins make it an ideal antimicrobial agent.

2.4.1   The Structures of Phage Endolysin

The endolysin structures are mainly influenced by their origin. For instance, the endolysins produced by the Gram-positive bacteria targeting phages have a molecular weight of 25−40 kDa (Liu, et al., 2023). These endolysins would most commonly consist of two modular structures, which are N-terminal enzymatically active domain (EAD) and C-terminal cell wall-binding domain (CBD), connected by a flexible linker (Hong, et al., 2019; Cernooka, et al., 2022; Liu, et al., 2023).

For instance, endolysin LysB4 consists of a VanY domain that serves as the EAD and a SH3_5 domain as the CBD (Hong, et al., 2019). Some of the endolysins contain two EADs that are linked to a CBD by the linkers like endolysin LysK. LysK is encoded by *S. aureus* phage K comprises of an N-terminal cysteine-histidine dependent amino-hydrolase/peptidase (CHAP) domain and a central amidase as the EADs, and a C-terminal SH3b cell-wall-binding domain as the CBD (Sanz-Gaitero, et al., 2014).

Conversely, Gram-negative bacteria targeting phages produce endolysins with a molecular weight of 15−20 kDa that have a simpler globular structure without CBD (Murray, et al., 2021; Liu, et al., 2023). LysECP26 is encoded by phage vB_EcoM-ECP26 which targets gram-negative bacteria, importantly *E.coli* O157:H7 (Park and Park, 2020). LysECP26 only consist of a single lysozyme-like catalytic domain. Besides, LysSTG2 derived from *Salmonella*-lytic bacteriophage STG2 also has an EAD, which hydrolyze the L-alanyl-D-glutamate peptide bond (Zhang, et al., 2021).

Interestingly, endolysins with signal-arrest-release (SAR) domain were identified (Abdelrahman, et al., 2021). These SAR endolysins can reach the peptidoglycan independent of holins. For example, Mu phage encodes a SAR endolysin that first translocates the endolysin into the periplasmic membrane through Sec pathway (Chamblee, et al., 2022). Then, the SAR endolysin is released into the periplasm to perform its catalytic activity.

2.4.2 Mechanism of Phage Endolysin Action

Peptidoglycan, is a crucial structure of the cell wall that withstands the turgor pressure and prevents the bursting of cells (Liu, et al., 2023). Various bonds formed in the polymerization of peptidoglycan are the cleavage targets of endolysin. In general, the N-terminal EAD functions to cleave the peptidoglycan bonds within the cell wall, while the C-terminal CBD binds specifically to the components of cell wall (typically carbohydrates and teichoic acids) through non-covalent bonding (Liu, et al., 2023). The sequence of CBD varies among the endolysins, giving rise to their species or strain specificity (Hong, et al., 2019; Liu, et al., 2023). Whereas, based on the functional group diversity in the EADs, EADs can be classified into three major classes, which are glycosidases, amidases, and enteropeptidases (Murray, et al., 2021).

Glycosidases can be further divided into N-acetyl-β-D-muramidases, which hydrolyze the β-1,4 glycosidic bonds found between N-acetylmuramic acids (NAM) and N-acetyglucosamines (NAG), and N-acetyl-β-D-glucosidases, which cleave the glycosidic bonds linking NAG and NAM (Murray, et al., 2021). Amidases, specifically known as N-acetylmuramoyl-L-alanine amidases,

function to break down the amide bond between the NAM and L-alanine residues, which usually links the glycan stand to the stem peptide (Murray, et al., 2021). Endopeptidases, which include L-alanoyl-D-glutamate endopeptidase, c-D-glutamyl-m-diaminopimelic acid peptidase, D-Ala-m-DAP endopeptidase, D-alanyl-glycyl endopeptidase, act by hydrolyzing the bonds between two respective amino acids found either within the interpeptide bridge or stem peptide-interpeptide bridge (Abdelrahman, et al., 2021). The overview of three major classes of enzymatic cleavage sites is shown in Figure 2.6.
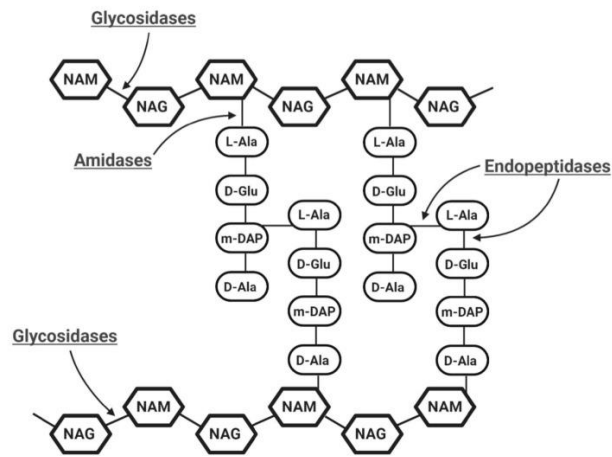
Figure 2.6: The overview of six enzymatic cleavage sites of glycosidases, amidases, and endopeptidases (Adapted from Abdelrahman, et al., 2021).

Therefore, the administration of endolysin leads to cleavage of the peptidoglycan from the external site of the bacteria. (Schmelcher and Loessner, 2021). This disrupts the cell wall integrity, thus increasing the intracellular osmotic pressure that results in cell death. Endolysins exhibit higher efficacy in combating gram-positive bacteria compared to gram-negative bacteria as the outer membrane of the gram-negative bacteria confers resistance towards

endolysins by preventing the access to peptidoglycan (Zhang, et al., 2022). The resistance can be overcome by the application of ethylenediaminetetraacetic acid (EDTA) which facilitates endolysins to reach the peptidoglycan by enhancing the outer membrane permeability (Zhang, et al., 2022).

2.4.3 Advantages of Recombinant Phage Endolysin

Phage therapy was first developed before the emergence of recombinant endolysins an alternative treatment. Studies have shown that recombinant endolysin is a better candidate than phage therapy as an antimicrobial agent.

Firstly, recombinant endolysins can effectively kill Gram-positive and negative bacteria, including the most virulent ESKAPE pathogens and disrupt their biofilm (Rahman, et al., 2021; Zhang, et al., 2022; Liu, et al., 2023). Beside ESKAPE pathogens, the recombinant endolysin also showed antibacterial and antibiofilm activities against other bacteria. For instance, phage vB_LmoS_293 endolysin could prevent the biofilm formation by *L. monocytogenes*, while artilysin lyses the *H. pylori*, which is the most common causative agent for gastric cancer (Pennone, et al., 2019; Xu, et al., 2021).

Secondly, recombinant endolysins have a broader bacterial host range than bacteriophages (Liu, et al., 2023). A study reported that SS3e phage was able to kill most of the *Salmonella* isolates and *Enterobacteriaceae*, but not able to lyse *K. pneumoniae*, *S. aureus*, *P. aeruginosa*, and *A. baumannii* (Kim, et al., 2018). However, the recombinant LysSS derived from SS3e phage could kill not only

those within the phage host-range, but also *K. pneumoniae*, *S. aureus*, *P. aeruginosa*, and *A. baumannii* (Kim, et al., 2020a).

Thirdly, phages are subjected to clearance by the immune systems as studies have identified the presence of anti-phage antibodies (Murray, et al, 2021). Although recombinant endolysin is immunogenic, the antibodies generated against the recombinant endolysin do not neutralize the endolysin (Liu, et al., 2023). Thus, the efficacy of the endolysin as an antimicrobial agent will not be affected. Notably, no resistance towards recombinant endolysin has been reported thus far, whereas phage therapy confers a low level of resistance by the bacterial cells (Liu et al., 2023).

On top of that, recombinant endolysins can be easily modified, enhancing its effectiveness. For example, removal of an amide-2 domain from PlyTW endolysin had enhanced its lytic efficiency (Becker, et al., 2015). A hybrid endolysin was synthesized from the fusion of LysB4 and LysSA11 (Son, et al., 2020). This hybrid endolysin LysB4EAD-LysSA11 was rapidly effective against *S. aureus* and *B. cereus*.

Besides these advantages, the antibiofilm activity of recombinant endolysin has been the focus of the research. Hence, there are many endolysins from either different phages have been cloned and engineered (Lu, et al., 2021; Rahman, et al., 2021; Wang, et al., 2021; Zhang, et al., 2022). These recombinant endolysins had shown great antibiofilm activity against various bacteria, including *S. aureus* and *P. aeruginosa*.

For instance, an *in-vivo* animal model study reported that endolysin LysECD7 derived from a mesophilic Escherichia phage ECD7, significantly reduced the biomass of biofilms formed by *K. pneumoniae* in a diffusion chamber (Fursov, et al., 2020). Furthermore, thermophilic endolysins encoded by thermophage from the hot springs also showed a broad antimicrobial activity (Liu, Kheirvari and Tumban, 2023).

In a food processing setting, contamination with biofilms is also one of the issues faced by the manufacturer (Galié, et al., 2018). In this circumstance, a thermophilic endolysin would be more stable and effective against the bacterial cells as compared to a mesophilic endolysin (Liu, Kheirvari and Tumban, 2023).

In this study, the antibiofilm activity of a novel recombinant endolysin derived from a hot spring thermophage was tested against *S. aureus* and *P. aeruginosa*.

CHAPTER 3

MATERIALS AND METHODS

3.1   Materials

3.1.1   Chemicals and Reagents

All the chemicals and reagents utilized in this project are listed in Appendix A.

3.1.2   Equipment and Laboratory Wares

All the equipment and laboratory wares utilized throughout this project are listed in Appendix B.

3.1.3   Bacterial Strains

The ATCC bacterial strains of *Staphylococcus aureus* (ATCC BAA-1026) and *Pseudomonas aeruginosa* (ATCC 27853) were obtained from Department of Biomedical Science, Faculty of Science, Universiti Tunku Abdul Rahman. *Escherichia coli* BL21 (DE3) was used as the host cell to express the his-tagged novel recombinant endolysin. The gene encoding for novel endolysin was originated from a novel *Escherichia* phage KW1E_UTAR (accession number MZ506873). The endolysin gene was cloned into an expression vector, pET-28a(+) and fused with a His-tag. This recombinant plasmid was then transformed into and expressed in *E. coli* BL21 (DE3) cells.

3.2 Optimization of Biofilm Formation

The *S. aureus* and *P. aeruginosa* biofilm formation was optimized by testing on different glucose concentrations, initial bacterial cell titers and incubation temperatures. The glucose concentrations tested were 0.25%, 0.5%, and 1.0%. Then, the bacterial cell titers in the initial inoculum tested were 10^4 CFU/mL, 10^5 CFU/mL, 10^6 CFU/mL, 10^7 CFU/mL, 10^8 CFU/mL, and 10^9 CFU/mL. The incubation temperatures tested were 25℃, 30℃, and 37℃.

3.2.1 Preparation of Luria Bertani (LB) Agar

Thirty-five grams of LB agar powder was added into 500 mL of deionized water and mixed well before autoclaving. Then, the autoclaved LB agar was allowed to cool to 55℃ and poured into sterile petri dishes and allowed to solidify. The LB agar plates were stored at 4℃ until use.

3.2.2 Preparation of Luria Bertani (LB) Broth

Ten grams LB broth powder was added into 500 mL of deionized water. The mixture was mixed well and autoclaved. Then, the autoclaved LB broth was stored at room temperature until use.

3.2.3 Preparation of 25% (v/v) Bacterial Glycerol Stock Solution

Twenty-five milliliters of 99.5% glycerol was dissolved in 25 mL of deionized water and autoclaved. The 50% glycerol solution was stored at room temperature. After that, the log-phase *S. aureus* and *P. aeruginosa* were prepared in LB broth before preserving them in 25% glycerol solution. The bacterial glycerol stock was stored at -80℃.

3.2.4 Preparation of Tryptic Soy Broth (TSB)

Twenty-four grams of TSB powder was added in 800 mL of deionized water. The mixture was mixed well and autoclaved before storing at room temperature until use.

3.2.5 Preparation of 20% (w/v) Glucose Stock Solution

Ten grams D-glucose was added into 50 mL of deionized water and mixed well. The glucose stock solution was filtered using a 0.45 µm syringe filter into a 50 mL media bottle. The 20% glucose solution was then kept at room temperature.

3.2.6 Preparation of Tryptic Soy Broth (TSB) Supplemented with 0.25% (v/v) Glucose

A total of 1.25 mL of 20% (v/v) glucose was mixed with 98.75 mL of TSB and kept at room temperature until use.

3.2.7 Preparation of Tryptic Soy Broth (TSB) Supplemented with 0.5% (v/v) Glucose

A total of 2.5 mL of 20% (v/v) glucose was mixed with 97.5 mL of TSB and kept at room temperature until use.

3.2.8 Preparation of Tryptic Soy Broth (TSB) Supplemented with 1.0% (v/v) Glucose

A total of 5 mL of 20% (v/v) glucose was mixed with 95 mL of TSB and kept at room temperature until use.

3.2.9   Effect of Glucose Concentration on Biofilm Formation

Firstly, the culture plates of *S. aureus* and *P. aeruginosa* were prepared on LB agar. Then, the inoculums of both bacteria were grown overnight in TSB at 37°C with shaking at 200 rpm. The overnight cultures were diluted ten times using different glucose concentrations supplemented TSB (TSB + 0.25% glucose, TSB + 0.5% glucose and TSB + 1.0% glucose). These diluted inoculums were allowed to reach 0.6 at OD_{600}. Then, the inoculums were adjusted to 10^8 CFU/mL based on 0.5 McFarland using respective glucose concentration supplemented TSB. Then, 200 μL inoculum grown in TSB supplemented with different glucose concentrations was added into the 96-well plate. The same volume of the culture media without bacterial inoculation serving as negative control was added to the plate. The layout of the bacterial inoculums in a 96-well plate is illustrated in Figure 3.1. The plates containing *S. aureus* and *P. aeruginosa*, respectively, were incubated for 24 h at 37°C without agitation.
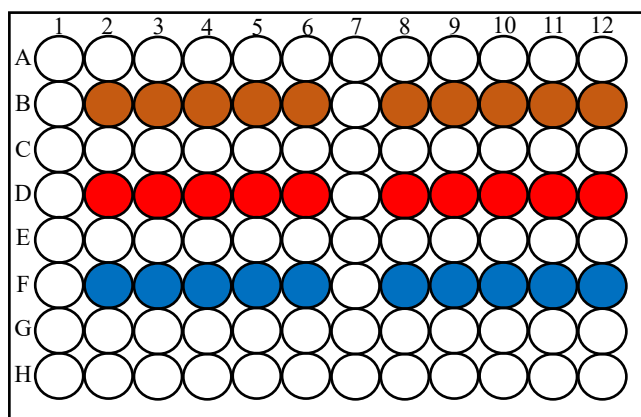
Figure 3.1: The arrangement of 96-well plate for optimization of glucose concentration. The log-phased inoculums were adjusted to 10^8 CFU/mL before being added to the wells. Wells B2-B6 were added with 200 µL of inoculums grown in TSB supplemented with 0.25% glucose and wells B8-B12 were added with 200 µL of TSB supplemented with 0.25% glucose without inoculums (Brown). Wells D2-D6 were added with 200 µL of inoculums grown in TSB supplemented with 0.5% glucose and wells D8-D12 were added with 200 µL of TSB supplemented with 0.5% glucose without inoculums (Red). Wells F2-F6 were added with 200 µL of inoculums grown in TSB supplemented with 1.0% glucose and wells F8-F12 were added with 200 µL of TSB supplemented with 1.0% glucose without inoculums (Blue). All the culture broths without the inoculums served as the negative control.

3.2.10 Effect of Initial Bacterial Cell Titer on Biofilm Formation

Then, TSB supplemented with 1.0% glucose was selected. After preparing *S. aureus* and *P. aeruginosa* overnight cultures in TSB supplemented with 1.0%, the cultures were diluted 10 times using the same culture medium and incubated at 37°C with shaking at 200 rpm until they reached 0.6 at OD_{600}. The inoculums were first adjusted to 10^9 CFU/mL based on 1.5 McFarland using the culture medium. Then, it was followed by 10-fold serial dilutions of 10^9 CFU/mL inoculums using the culture medium to prepare the initial inoculums of 10^4 CFU/mL - 10^8 CFU/mL. After that, 200 µL inoculum from each initial bacterial cell titer (10^4 CFU/mL – 10^9 CFU/mL) was added into the wells of a 96-well plate. The same volume of the culture medium without bacterial inoculation

serving as negative control was added to the plate. The layout of the bacterial inoculums in a 96-well plate is shown in Figure 3.2. The plates containing *S. aureus* and *P. aeruginosa*, respectively, were incubated for 24 h at 37°C without agitation.
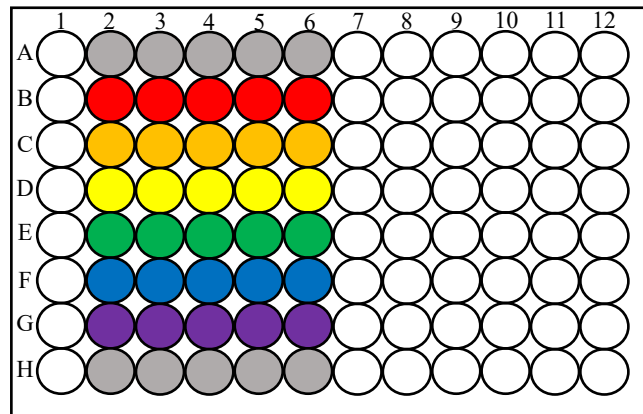
Figure 3.2: The arrangement of 96-well plate for optimization of initial bacterial cell titer. The initial inoculums ranging from 10^4 CFU/mL to 10^8 CFU/mL were prepared and added to the wells. Wells B2-B6 were added with 200 µL of 10^9 CFU/mL inoculums (Red). Wells C2-C6 were added with 200 µL of 10^8 CFU/mL inoculums (Orange). Wells D2-D6 were added with 200 µL of 10^7 CFU/mL inoculums (Yellow). Wells E2-E6 were added with 200 µL of 10^6 CFU/mL inoculums (Green). Wells F2-F6 were added with 200 µL of 10^5 CFU/mL inoculums (Blue). Wells G2-G6 were added with 200 µL of 10^4 CFU/mL inoculums (Purple). Wells A2-A6 and H2-H6 were added with TSB supplemented with 1.0% glucose without the inoculums (Grey), which served as the negative control.

3.2.11 Effect of Incubation Temperature on Biofilm Formation

According to the results, the selected initial bacterial cell titer is 10^8 CFU/mL. The overnight cultures of *S. aureus* and *P. aeruginosa* were diluted 10 times in TSB supplemented with 1.0% glucose. The inoculums were allowed to grow to 0.6 at OD_{600} by incubating at 37°C with shaking at 200 rpm. Then, the

inoculums were adjusted to 10^8 CFU/mL based on 0.5 McFarland using the culture medium. After that, 200 µL inoculum was added into the 96-well plate. The same volume of TSB supplemented with 1.0% glucose only (negative control) was added to the plate. Figure 3.3 shows the layout of the bacterial inoculums in a 96-well plate. Three plates with the same layout shown in Figure 3.3 were prepared for each bacteria. The plates containing *S. aureus* and *P. aeruginosa* were incubated at 25°C, 30°C and 37°C, respectively, for 24 h.
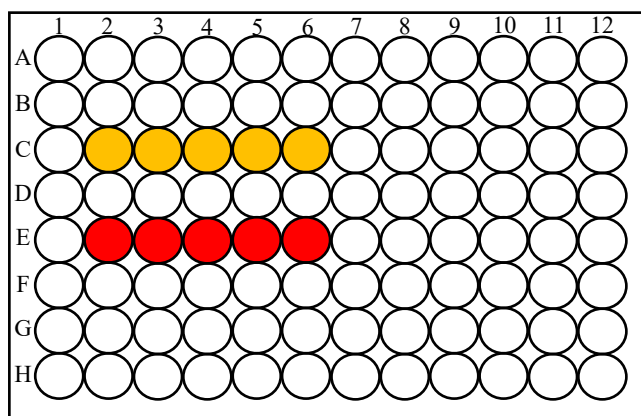
Figure 3.3: The arrangement of 96-well plate for optimization of incubation temperature. Wells C2-C6 were added with 200 µL of inoculums (orange) and wells E2-E6 were added with 200 µL of culture medium with inoculum as the negative control (red). Six plates of this with 3 plates for each bacteria were incubated at room temperature, 30°C and 37°C, respectively.

3.3   Crystal Violet Assay

3.3.1   Preparation of 0.1% (v/v) Crystal Violet (CV) Solution

Ten milliliters of 0.5% CV solution was added into 40 mL of deionized water. The 0.1% CV solution was stored in a centrifuge tube covered with aluminum foil at room temperature.

3.3.2   Preparation of 33% (v/v) Acetic Acid

Thirteen point two milliliters of glacial acetic acid was added in 26.8 mL of deionized water. The 33% acetic acid was kept at room temperature.

3.3.3   Preparation of 70% (v/v) Ethanol

A total volume of 737 mL ethanol was dissolved in 263 mL of deionized water. The 70% ethanol was stored at room temperature.

3.3.4   Preparation of Phosphate Buffered Saline (PBS), pH 7.4

A total of 4.4 g sodium dihydrogen phosphate and 9 g disodium phosphate were weighed and dissolved in 800 mL of deionized water. The pH of the solution was adjusted to pH 7.4 with 0.1 M sodium hydroxide. Then, the solution was topped up to 1 L with deionized water and autoclaved. The solution was then stored at room temperature.

3.3.5   Crystal Violet (CV) Staining

After incubation, the supernatant in the wells containing the planktonic cells was discarded. The wells were washed thrice with 200 µL of PBS (pH 7.4). The biofilms formed were fixed by heating at 60°C for 1 h. Subsequently, 200 µL of

0.1% (v/v) CV solution was added into each well and incubated at room temperature. After 20 min of incubation, the excess CV solution in the wells was discarded and the wells were then washed thrice with 200 µL of PBS. The 96-well plates were allowed to air dry for 30 min at room temperature. The plate inoculated with *S. aureus* was added with 200 µL of 33% acetic acid to solubilize the CV stain whereas 200 µL of 70% ethanol was used to solubilize the CV stain for the plate inoculated with *P. aeruginosa*. The absorbance of the solubilized CV was read at OD_{595} using a microplate reader.

3.3.6 Evaluation of Biofilm Formation

The biofilm formed was categorized into four groups based on the cut-off values as stated by Extremina, et al. (2011). The cut-off value (ODc) refers to the average OD of the negative control (ODnc)

The average OD values were calculated for all tested strains and negative controls (nc) and the cut-off value (ODc) was established. ODc was calculated by the addition of the mean OD of the negative control (ODnc) to three standard deviation of the negative control (SDnc) [ODc= mean ODnc+(3×SDnc)]. The bacteria that form biofilms with: OD ≤ ODc are non biofilm producers, ODc < OD ≤ 2×ODc are weak biofilm producers, 2×ODc < OD ≤ 4×ODc are moderate biofilm producers and 4×ODc < OD are strong biofilm producers.

3.4 Expression of Recombinant Phage Endolysin

3.4.1 Preparation of 35 mg/mL Kanamycin Stock Solution

A total of 1.75 g of kanamycin was added into 50 mL of deionized water and mixed well. The kanamycin solution was filtered using a 0.22 μm syringe filter and stored at -20°C.

3.4.2 Preparation of *E. coli* BL21 (DE3) Glycerol Stock

The single colony of *E. coli* BL21 (DE3) containing plasmid harboring the gene encoding for his-tagged endolysin was cultivated in LB broth. Then, 200 μL of culture was added into 200 μL of 50% glycerol solution to prepare a final concentration of 25%. Then, the glycerol stock was kept at -80°C.

3.4.3 Preparation of LB Agar Supplemented with 35 μg/mL

Seven grams of LB agar powder was added into 200 mL of deionized water and mixed well before autoclaving. Then, the autoclaved LB agar was allowed to cool to 55°C. After that, 200 μL of 35 mg/mL kanamycin solution was added into the LB agar to a final concentration of 35 μg/mL. The agar was mixed well before pouring it into sterile petri dishes. The agars were allowed to solidify before storing them at 4°C.

3.4.4 Preparation of 100 mM Isopropyl B-D-1-Thiogalactopyranoside (IPTG) Stock Solution

A total of 0.238 g IPTG was weighed and dissolved in 10 mL of deionized water. The solution was mixed well and filtered using a 0.22 μm syringe filter. The IPTG solution was then stored at -20°C until use.

3.4.5   Expression of Recombinant Phage Endolysin

Escherichia coli BL21 (DE3) harboring the gene encoding for his-tagged novel endolysin were grown overnight in LB broth (pH 7.0) containing 35 µg/mL kanamycin at 37℃ with shaking at 200 rpm. The overnight culture of the *E. coli* cells was then diluted with the same broth in a 1:50 ratio and incubated at 37℃ with shaking at 200 rpm. Once OD_{600} reached 0.6, the expression of the target endolysin gene was induced by adding IPTG to a final concentration of 0.5 mM. The culture was then incubated overnight at 18℃ with shaking at 200 rpm.

3.4.6   Preparation of 20 mM Sodium Phosphate Buffer Containing 300 mM NaCl, pH 7.4

A total volume of 100 mL of 0.1 M disodium phosphate was measured and dissolved in 200 mL of deionized water. Then, 0.1 M sodium dihydrogen phosphate was used to adjust the pH to 7.4. After that, 8.766 g of sodium chloride was weighed and dissolved in the buffer, and then, the buffer was added up to 500 mL. The buffer was autoclaved and stored at room temperature.

3.4.7   Preparation of Lysis Buffer

A total of 30 mg lysozyme was dissolved in 30 mL of 20 mM sodium phosphate buffer to obtain a final concentration of 1 mg/mL. The solution was mixed well.

3.4.8   Harvesting of Recombinant Phage Endolysin

On the next day, the culture was centrifuged at 10000 rpm for 20 min at 4℃. The harvested cells were suspended in 30 mL of 20 mM sodium phosphate buffer containing 1 mg/mL lysozyme (lysis buffer) and placed on ice. The suspended cells were disrupted through sonication for 1 h and 30 min. The

resulted cell lysate was then centrifuged at 10,000 rpm for 30 min at 4°C. The supernatant was collected and filtered using a 0.45 µm syringe filter.

3.5 Purification of Recombinant His-tagged Endolysin

3.5.1 Preparation of Binding Buffer

A total of 0.163 g of imidazole was weighed and dissolved in 60 mL sodium phosphate buffer to prepare a final molarity of 40 mM. The solution was then mixed well.

3.5.2 Preparation of Elution Buffer

A total of 1.532 g of imidazole was weighed and dissolved in 30 mL sodium phosphate buffer to prepare a final molarity of 750 mM. The solution was then mixed well.

3.5.3 Preparation of 0.1 M Nickel Sulfate

A total of 2.629 g nickel sulfate hexahydrate was dissolved in 100 mL of deionized water and mixed well before storing it at 4°C.

3.5.4 Purification of Recombinant His-tagged Endolysin

The recombinant endolysin in the supernatant obtained in Section 3.4.8 was purified with nickel affinity chromatography. The column was first packed with Ni resins and followed by recharge of 25 mL of nickel using 0.1M nickel sulphate. After equilibrating the column with 100 mL of 20 mM sodium phosphate buffer containing 300 mM NaCl, the supernatant containing recombinant his-tagged endolysin was added to the column. Then, 60 mL of

binding buffer (20 mM sodium phosphate buffer, 300 mM NaCl and 40 mM imidazole) was added to remove unbound proteins from the column. After that, 30 mL of elution buffer (20 mM sodium phosphate buffer, 300 mM NaCl and 750 mM imidazole) was added to elute the recombinant his-tagged endolysins. All flowthroughs from the column were collected in fractions which were analyzed by sodium dodecyl sulfate-polyacrylamide gel electrophoresis (SDS-PAGE).

3.6 Sodium dodecyl sulfate-polyacrylamide gel electrophoresis (SDS-PAGE).

3.6.1 Preparation of Acrylamide Mix (30% T, 2.67% C)

Twenty-nine point two grams of acrylamide and zero point eight grams of bis-acrylamide were added into 100 mL deionized water and mixed well. Then, the solution was filtered using 0.45 μm syringe filter and stored in an amber media bottle at 4°C.

3.6.2 Preparation of 10% (w/v) Sodium Dodecyl Sulfate (SDS)

Ten grams of SDS was added into 100 mL deionized water and mixed well before filtering using 0.22 μm syringe filter. The solution was stored at room temperature until use. The SDS solution was heated at 65°C to solubilize the precipitates before use.

3.6.3 Preparation of 4X Lower Buffer, pH 8.8

A total of 18.171 g tris base powder was dissolved in 40 mL deionized water to prepare a final concentration of 1.5 M. A concentrated hydrochloric acid (37%) was used to adjust the pH to 8.8 with. Then, 4 mL of 10% SDS was measured

and added to the solution to obtain a final concentration of 0.4%. The buffer was added up to 100 mL with deionized water and stored at 4°C without autoclaving.

3.6.4   Preparation of 4X Upper Buffer, pH 6.8

A total of 6.057 g tris base powder was added into 30 mL deionized water to prepare a final molarity of 0.5 M. The pH was adjusted to pH 6.8 with concentrated hydrochloric acid. Then, 4 mL of 10% SDS was measured and added to the solution to obtain a final concentration of 0.4%. The upper buffer was added up to 100 mL with deionized water and stored at 4°C without autoclaving.

3.6.5   Preparation of 10% Ammonium Persulfate (APS)

One gram of APS was added into 10 mL of deionized water to yield a final concentration of 10% and mixed well before storing it at -20°C.

3.6.6   Preparation Resolving and Stacking Gels

The resolving was prepared as mentioned in Table 3.1 and added into the gel casting. N-butanol was quickly layered on top of the resolving gel. After the gel had solidified, N-butanol was removed and the gel was rinsed with water. Then, the stacking gel was prepared as mentioned in Table 3.1 and added on top of the resolving gel. The comb was quickly inserted into the stacking gel and the gel was allowed to solidify.

Table 3.1: Resolving and stacking gels preparation.

Reagents	Stacking gel (5%)	Resolving gel (15%)
30% Acrylamide mix	625 μL	3.75 mL
Deionized water	2.19 mL	1.88 mL
4X Lower buffer	-	1.88 mL
4X Upper buffer	940 μL	-
10% APS	17.5 μL	47 μL
TEMED	5.3 μL	7.5 μL

3.6.7 Preparation of 2X Sample Loading Buffer (SAB)

The 0.5 M tris buffer was first prepared by dissolving 0.3023 g Tris-HCl powder in 5 mL of deionized water. A concentrated sodium hydroxide (pellet) was used to adjust the pH to 6.8. The sample loading buffer without β-mercaptoethanol was prepared as mentioned in Table 3.2. The mixture was mixed well and then equally aliquoted into 10 microcentrifuge tubes shielded with aluminum foil and kept at room temperature. A total of 100 μL of β-mercaptoethanol was added into one of the sample loading buffers and mixed well before use.

Table 3.2: Sample loading buffer preparation.

Reagents	Initial concentration	Final concentration	Volume/ amount
Tris buffer (pH 6.8)	0.5 M	0.15 M	3 mL
SDS	10%	4%	4 ml
Glycerol	99.5%	20%	2 mL
Bromophenol blue	-	0.06%	6 mg
β-mercaptoethanol	99%	10%	1 mL
Total			10 mL

3.6.8 Preparation of Sample

A total of 6 mL of SAB was added to 6 mL of protein samples. The mixture was mixed well and heated at 95°C for 10 min.

3.6.9   Preparation of 10X Running Buffer (without SDS)

A total of 15 g tris-base and 72 g glycine were added into 500 mL deionized water and mixed well and stored in a media bottle covered with aluminum foil at room temperature.

3.6.10 Preparation of 1X Running Buffer

A total of 100 mL of 10X running buffer was diluted in 890 mL of deionized water to obtain a final concentration of 1X. Then, 10 mL of 10% SDS was added to the solutions.

3.6.11 SDS-PAGE

The solidified gels with the combd removed were immersed in 1X running buffer in a gel tank. The prepared samples were loaded into the wells. The gel electrophoresis was run at 32 mA for 1 h.

3.6.12 Preparation of Staining Solution

A total of 0.5 g of Coomassie brilliant blue G250 was weighed and dissolved in 150 mL methanol (final concentration of 30%). Then, 325 mL deionized water and 25 mL glacial acetic acid were measured and added to the mixture (final concentration of 5%). The solution was mixed well and filtered using the Whatman No. 1 paper. The staining solution was stored in a media bottle covered with aluminum foil at room temperature.

3.6.13 Preparation of Destaining Solution

A total of 200 mL methanol (final concentration of 40%) was measured and added into 250 mL of deionized water. Then, 50 mL of glacial acetic acid (final concentration of 10%) was measured and added into the solution. The solution was mixed well and stored at room temperature.

3.6.14 Visualization of Gel

After electrophoresis, the gel was stained with the staining solution for 5 min and destained with the destaining solution for 2 h. Then, the gel was visualized using a gel imager.

3.7   Pooling of Purified Recombinant Endolysin Protein

3.7.1   Preparation of 20 mM Sodium Phosphate Buffer Containing 150 mM NaCl (Desalting Buffer), pH 7.4

A total volume of 100 mL of 0.1 M disodium phosphate was added into 500 mL of deionized water and 0.1 M sodium dihydrogen phosphate was used to adjust the pH to 7.4. Then, 8.766 g of sodium chloride was weighed, dissolved in the solution, and topped up to 1 L with deionized water. The solution was autoclaved and stored at room temperature.

3.7.2   Pooling and Dialysis of Purified Recombinant Endolysin Protein

The snakeskin dialysis membrane tubing with 10 kDa molecular weight cut-off (MWCO) and a length of 10 cm was prepared. Fractions containing the recombinant endolysin were added into dialysis tubing, then placed into a beaker containing desalting buffer (pH 7.4). After that, the protein was dialyzed

overnight at 4°C. The desalting buffer was changed atleast 3 times for every 2 h of dialysis.

The dialyzed protein was concentrated through an ultrafiltration membrane with a MWCO of 10 kDa by centrifuging at 5400 rpm for 10 min at 20°C. The concentration recombinant endolysin was quantified using the Bradford protein assay and stored at 4°C.

3.8 Bradford Protein Assay

3.8.1 Preparation of 2 mg/mL Bovine Serum Albumin (BSA) Stock Solution

Ten milligrams of BSA powder was dissolved in 5 mL of deionized water. The standard BSA solution was stored at 4°C.

3.8.2 Preparation of BSA Standard Curve

A series of dilutions using 2 mg/mL BSA solution was prepared as mentioned in Table 3.3. The 20 mM sodium phosphate buffer containing 150 mM NaCl was used as the diluent. Then, 20 μL of each standard dilution and protein samples were mixed with 1 mL of Bradford reagent. The standard dilutions and samples were then stood for 5 min at room temperature. After that, OD_{595} was measured and a BSA standard curve was plotted as shown in Figure 3.4. The OD_{595} values of the unknown protein samples was compared to the BSA standard curve to quantify the concentration of the protein samples.

Table 3.3: BSA standards preparation.

Tube	BSA concentration ($\mu g/mL$)	Volume of BSA standard solution (μL)	Volume of diluent (μL)
A	2000	200	-
B	1500	150 from Tube A	50
C	1000	133 from Tube B	67
D	500	100 from Tube C	100
E	250	100 from Tube D	100
F	125	100 from Tube E	100
G	0	-	200

Note. 20 mM sodium phosphate buffer containing 150 mM NaCl was used as the diluent.
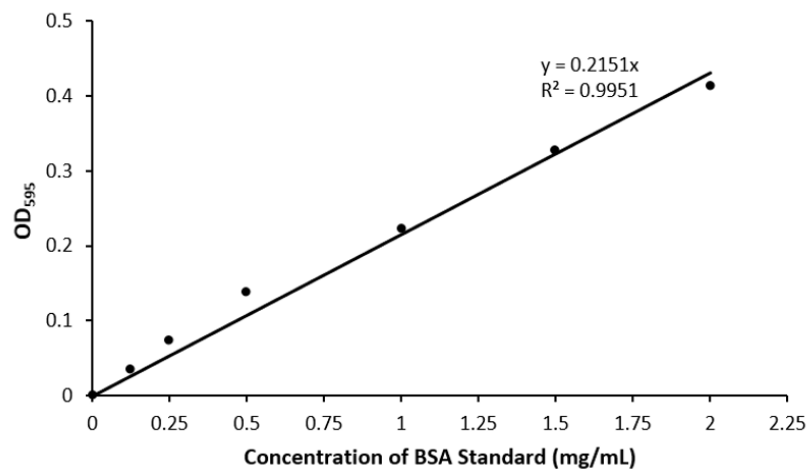
Figure 3.4: Bradford assay standard curve of concentration versus absorbance. The concentration of protein samples was determined using the equation y = 0.2151x with a strong R^2 value of 0.9951.

The quantified protein was diluted in a 2-fold serial dilution with 20 mM sodium phosphate buffer containing 150 mM NaCl to prepare a set of 11 concentrations – 1000 $\mu g/mL$, 500 $\mu g/mL$, 250 $\mu g/mL$, 125 $\mu g/mL$, 62.5 $\mu g/mL$, 31.25 $\mu g/mL$, 15.625 $\mu g/mL$, 7.813 $\mu g/mL$, 3.906 $\mu g/mL$, 1.953 $\mu g/mL$, 0.977 $\mu g/mL$ of endolysins.

3.9 Preparation of 500 mM Ethylenediaminetetraacetic acid (EDTA)

A total of 7.306 g of EDTA was weighed and dissolved in 40 mL of deionized water. The pH of the mixture was adjusted to pH 8.0 by adding pellets of sodium chloride. Then, the deionized water was added to the solution to obtain afinal volume of 50 mL. The solution was autoclaved and kept at room temperature.

3.10 Biofilm Inhibition Assay

Based on the results obtained from the optimization of biofilm formation (Section 3.3.1), TSB supplemented with 1.0% glucose, 10^8 CFU/mL (McFarland standard 0.5) and 37°C were selected as the culture medium, bacterial titer in the initial inoculum and incubation temperature, respectively, for the formation of biofilm. The biofilm inhibition assay was conducted with some modification from previous study (Haney, Trimble and Hancock, 2021). Overnight cultures of *S. aureus* and *P. aeruginosa* in TSB were prepared and diluted in the assay medium in a 1:10 ratio. The diluted cultures were allowed to grow to log phase (OD_{600} of 0.6-0.65) before diluting them to 10^8 CFU/mL with the culture medium.

Then, 200 µL of the inoculums and 100 µL of increasing concentrations of endolysins (0.977 µg/mL to 1000 µg/mL) were inoculated into the wells of 96 wells microtiter plates. Besides, 200 µL of inoculums without the endolysin treatment (negative control) and culture medium without the inoculum (blank) were added into the wells, respectively. For gram-negative bacteria, *P. aeruginosa*, was added with EDTA to a final concentration of 5 mM. The layout of the 96-well microtiter plate is illustrated in Figure 3.5. The microtiter plates

were then incubated at 37°C for 24 h. After incubation, CV staining was performed as mentioned in Section 3.3.5 to quantify the biofilm formation.
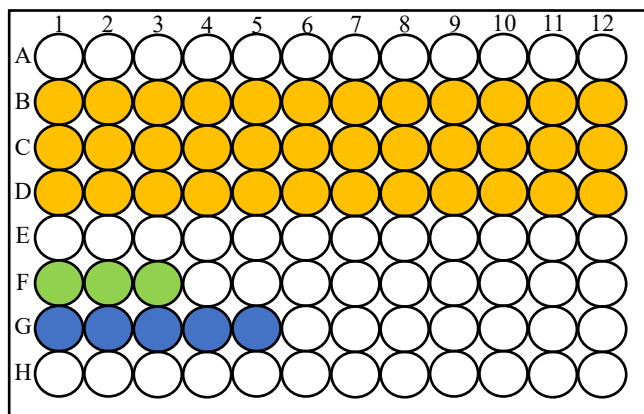
Figure 3.5: The arrangement of 96-well layplate for biofilm inhibition assay. Wells of rows B to D were added with bacterial inoculums, as represented in yellow. Then, wells B2 to B12, C2 to C12, and D2 to D12 were added with increasing concentrations of endolysin ranging from 0.977 µg/mL to 1000 µg/mL, respectively, while wells B1, C1, and D1 were added with the desalting buffer. Wells F1 to F3, which are green in color, were added with bacterial inoculums without the endolysin treatment, which acted as the negative control. The blue wells G1 to G5 were added with uninoculated TSB supplemented with 1.0% glucose, serving as blank.

The percentage of biofilm inhibition was calculated using the following formula (Haney, Trimble and Hancock, 2021):

$$\text{Percentage of biofilm inhibition} = \left(1 - \frac{\text{OD}_{595} \text{ treated sample-Blank}}{\text{OD}_{595} \text{ negative sample-Blank}}\right) \times 100\%$$

3.11   Biofilm Eradication Assay

The biofilm eradication assay was conducted with some modifications from previous study (Haney, Trimble and Hancock, 2021). The overnight cultures of *S. aureus* and *P. aeruginosa* in TSB were prepared and diluted in the selected culture medium, as described in Section 3.9. Once the cultures reached 0.6-0.65 at OD_{600}, they were diluted to 10^8 CFU/mL with the culture medium and 200 µL of inoculums were added into the 96-well microtiter plate based on the layout shown in Figure 3.6. The same volume of culture medium without the inoculums was added to the plate (blank). The plates were incubated at 37°C for 24 h to allow the formation of mature biofilms.
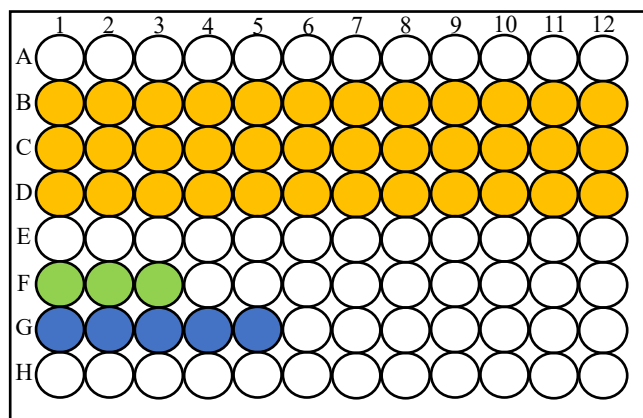
Figure 3.6: The arrangement of a 96-well plate for biofilm eradication assay. Wells of rows B to D were added with bacterial inoculums, as represented in yellow. Wells F1 to F3, which are green in color, were also added with bacterial inoculums, which acted as the negative control. The blue wells G1 to G5 were added with culture medium, which served as the blank. After 24 h of incubation, the supernatant in the wells was removed and washed. Then, wells B2 to B12, C2 to C12, and D2 to D12 were added with increasing concentrations of endolysin that ranged from 0.977 µg/mL to 1000 µg/mL, respectively, while wells B1, C1, and D1 were added with 20 mM sodium phosphate buffer containing 150 mM NaCl without the endolysin.

After 24 h, the supernatant containing the planktonic cells was removed from the wells, and wells were washed twice with 400 µL of PBS to remove the remaining planktonic cells. After that, 100 µL of endolysin with increasing concentrations ranging from 0.977 to 1000 µg/mL, were added to the wells where the biofilms have been formed. Ethylenediaminetetraacetic was added into the wells containing *P. aeruginosa* to a final concentration of 5 mM. The microtiter plates were incubated at 37°C for 24 h. The next day, CV staining was performed as mentioned in Section 3.3.5 to quantify the biofilm that remained adhered to the plates.

The percentage of biofilm eradication was calculated using the following formula (Haney, Trimble and Hancock, 2021):

$$\text{Percentage of biofilm eradication} = \left(1 - \frac{\text{OD}_{595} \text{ treated sample-Blank}}{\text{OD}_{595} \text{ negative sample-Blank}}\right) \times 100\%$$

3.12 Statistical Analysis

Two independent experiments with 5 replicates in each independent experiment were carried out for each parameter in biofilm optimization.Two independent experiments with triplicates in each independent experiment were carried out for biofilm inhibition and eradication. The mean values and standard deviations for the degree of biofilm formation (in biofilm optimization), biofilm inhibition and eradication were calculated. The statistical differences between the outcomes obtained for each parameter in biofilm optimization, and between the non-treated biofilm and biofilm treated with recombinant endolysins were analyzed using one-way ANOVA test. The values were considered significantly different if the *p*-value was less than 0.05 ($p < 0.05$).

CHAPTER 4

RESULTS

4.1 Optimization of Biofilm Formation

In this study, the ability of the biofilm formation by *S. aureus* and *P. aeruginosa* was evaluated and optimized before conducting the antibiofilm assays. Several parameters were optimized, such as glucose concentration, initial bacterial cell titer, and incubation temperature, to achieve moderate to strong biofilm formation by both bacteria.

4.1.1 Effect of Glucose Concentration on Biofilm Formation

Three different glucose concentrations were tested on the biofilm formation. The biofilms were grown on Tryptic soy broth (TSB) supplemented with 0.25%, 0.5%, or 1.0% (v/v) glucose.

Staphylococcus aureus was a moderate to strong biofilm producer when it was cultured in TSB supplemented with 0.25%, 0.5% and 1.0% (v/v) glucose. The biofilm mass formed by *S. aureus* increased when the glucose concentration supplemented in TSB increased from 0.25 to 1.0%, as depicted in Figure 4.1(A). TSB supplemented with 1.0% glucose strongly promoted the production of robust biofilms as compared to 0.25% and 0.5% glucose whereby the mean absorbance value was significantly 2.7 and 2 folds higher than 0.25% and 0.5% ($p < 0.05$), respectively. This is indicated by the highest intensity of the crystal violet (CV), as observed in well number 5 (Figure 4.1 (B)).

(A)

(B)

Wells: 1   2   3   4   5   6
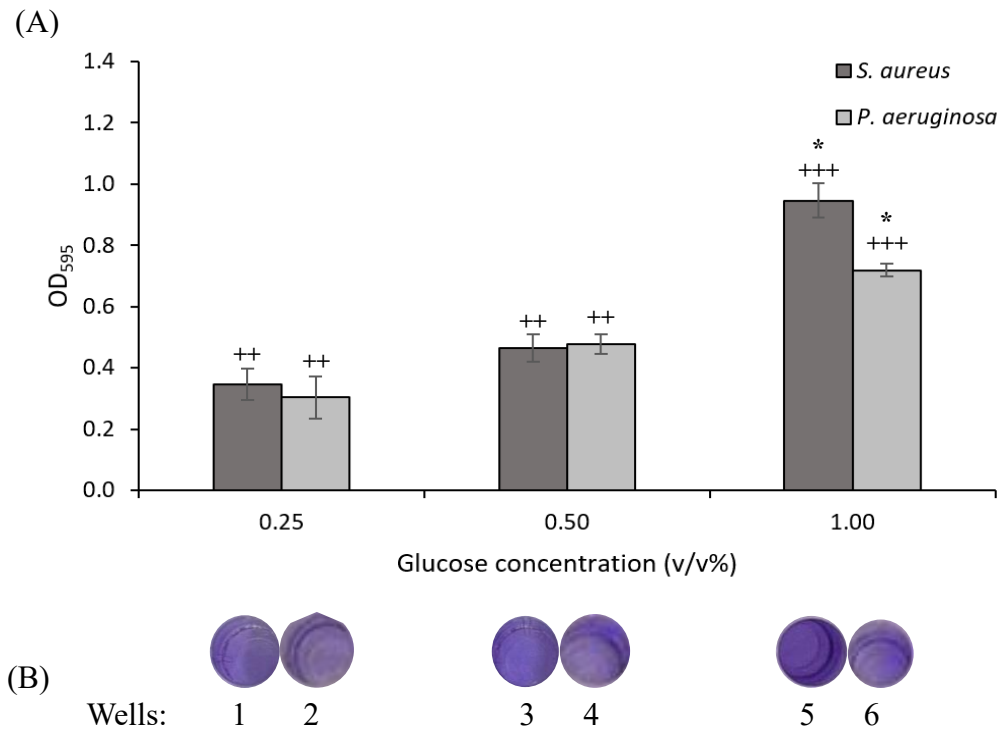
Figure 4.1: The biofilm mass formed by *S. aureus* and *P. aeruginosa* cultured in TSB supplemented with 0.25%, 0.50%, and 1.0% glucose. (A) Data are presented as mean and the error bars represent the standard deviation of triplicates. The classification of biofilms was denoted by the plus symbol – moderate biofilm producer (++) and strong biofilm producer (+++). The asterisks (*) indicate the significant differences between the glucose concentrations ($p < 0.05$). (B) The intensity of CV staining in wells which corresponds to the glucose concentrations.

Similarly, *P. aeruginosa* formed an increasing biofilm mass with increased in glucose concentration, as shown in Figure 4.1(A). *Pseudomonas aeruginosa* was a strong biofilm producer when TSB was supplemented with 1.0% (v/v) glucose. Based on the mean absorbance value, the mass of the biofilm produced in 1.0% glucose supplementation was significantly higher than 0.25% and 0.5%, by 2.3 and 1.5 folds ($p < 0.05$), respectively.

These results showed that both bacteria were strong biofilm producers when the culture medium was supplemented with 1.0% glucose. Therefore, TSB supplemented with 1.0% glucose was selected to proceed with the optimization of the following parameters.

4.1.2   Effect of Initial Bacterial Cell Titer on Biofilm Formation

The initial bacterial cell titers ranging from 10^4 to 10^9 CFU/mL, were evaluated on the biofilm formation by *S.aureus* and *P.aeruginosa*.

An increasing trend in the biofilm mass formation by *S. aureus* was observed when the initial bacterial cell titer was increased from 10^4 to 10^8 CFU/mL, as indicated by the increased mean absorbance values in Figure 4.2(A). No significant differences were observed between these initial bacterial titers ($p > 0.05$). Based on the mean absorbance values for these bacterial cell titers, *S. aureus* could be classified as a strong biofilm producer. However, when the initial bacterial cell titer was further increased to 10^9 CFU/mL, the biofilm mass formed was significantly reduced by 2 folds ($p < 0.05$) in comparison to 10^8 CFU/mL. Besides, the CV intensity in well number 11 (10^9 CFU/mL) was lower than that observed in well number 9 (10^8 CFU/mL) in Figure 4.2(B), which also indicated the reduction in the biofilm formed by 10^9 CFU/mL of *S. aureus*.

On the other hand, initial bacterial cell titers ranging from 10^4 to 10^7 CFU/mL increased the biofilm formed by *P. aeruginosa*, as shown by the increased mean absorbance values in Figure 4.2(A). However, the differences between these bacterial cell titers were insignificant ($p > 0.05$). The biofilm mass produced by

P. aeruginosa showed a significant increase ($p < 0.05$) of 44% when the initial bacterial cell titer was increased to 10^8 CFU/mL and this can be further supported by the higher CV intensity in well number 10, as depicted in Figure 4.2 (B). Moreover, *P. aeruginosa* was observed as a strong biofilm producer when an initial bacterial cell titer of 10^8 CFU/mL was used. Further bacterial cell titer increased to 10^9 CFU/mL has led to a significant drop in biofilm formation ($p < 0.05$), as seen in the decrease in mean absorbance value and intensity of CV staining in well number 12.

(A)

(B) Wells: 1 2 3 4 5 6 7 8 9 10 11 12
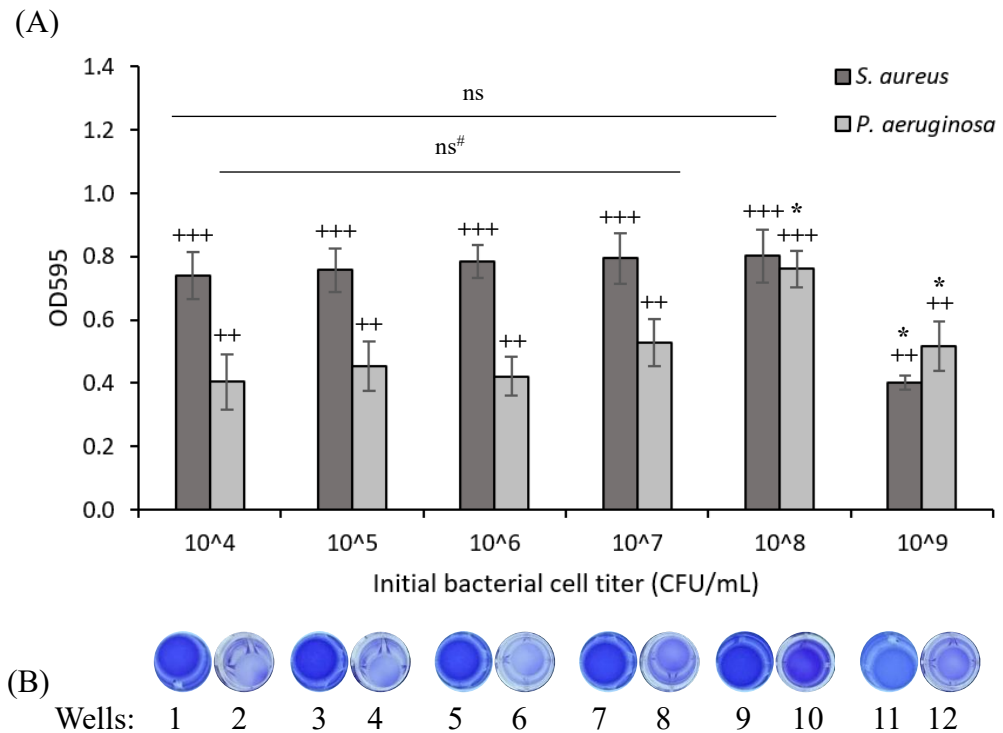
Figure 4.2: The effect of different initial bacterial cell titers on the biofilm mass formed by *S. aureus* and *P. aeruginosa*. (A) Data are presented as mean and the error bars refer to the standard deviation of triplicates. The classification of biofilms was denoted by the plus symbol – moderate biofilm producer (++) and strong biofilm producer (+++). "ns" denotes no significant difference observed for *S. aureus* and "ns#" denotes no significant difference observed for *P. aeruginosa* with $p > 0.05$. The asterisks (*) indicate the significant difference between the initial bacterial cell titers ($p < 0.05$). (B) The intensity of CV staining in wells which corresponds to the initial bacterial cell titers.

In summary, both *S.* aureus and *P. aeruginosa* were strong biofilm producers when 10^8 CFU/mL was used as the initial bacterial cell titer. Therefore, 10^8 CFU/mL was chosen to continue with the optimization of the next parameter.

4.1.3 Effect of Incubation Temperature on Biofilm Formation

Three incubation temperatures, which include 27°C, 30°C and 37°C, were evaluated for the optimum biofilm formation by *S. aureus* and *P. aeruginosa*.

Figure 4.3(A) shows that the biofilm mass formed by *S. aureus* was directly proportional to the incubation temperature. A higher temperature (37°C) has greatly enhanced the formation of robust biofilms, as seen by the significantly higher ($p < 0.05$) mean absorbance value of 37°C compared to 25°C and 30°C, as well as by the highest CV intensity in well number 5 (Figure 4.3(B)). Therefore, *S. aureus* was the strongest biofilm producer when cultivated at 37°C compared to lower temperatures at 25°C and 30°C.

In contrast, *P. aeruginosa* was a strong biofilm producer regardless of the temperatures (27°C, 30°C and 37°C) used. However, the biofilm mass formation decreased with the increasing incubation temperature, as illustrated in Figure 4.3(A). It was clearly shown that significant biofilm formation was observed at 27°C and this was evidenced by the highest CV intensity as observed in well 2 (Figure 4.3(B)). The biofilm mass was significantly reduced ($p < 0.05$) by 41% and 62% when the incubation temperature increased from 27 to 30 and 37°C, respectively.

55

(A)

(B) Wells: 1 2   3 4   5 6
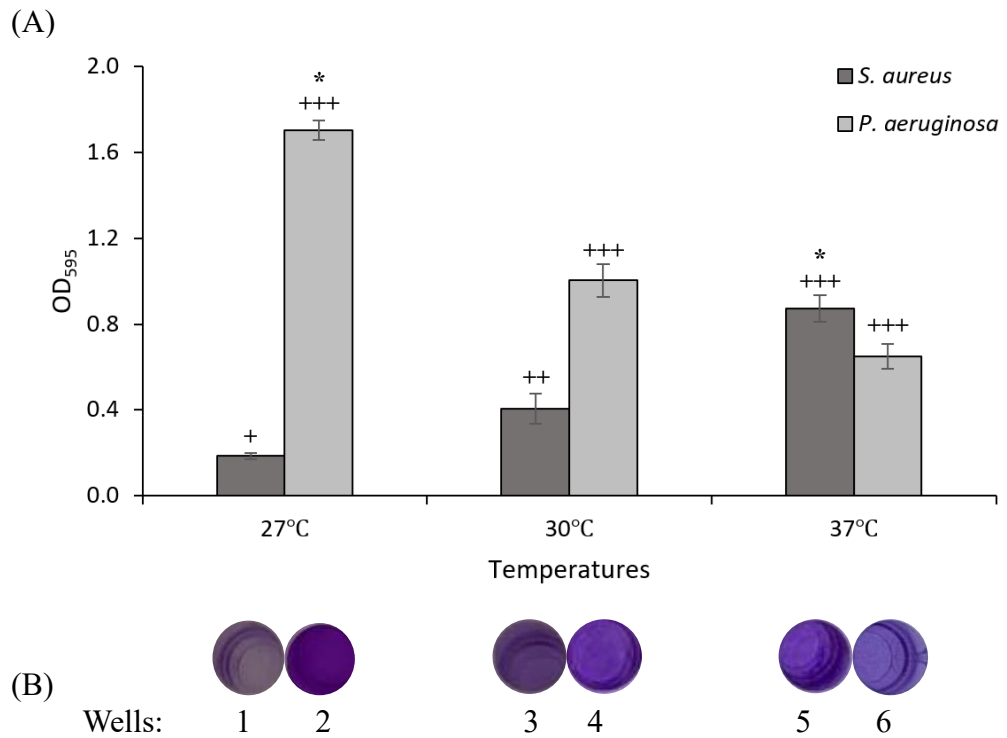
Figure 4.3: The effect of different incubation temperatures, 27°C, 30°C, and 37°C, on the biofilms produced by *S. aureus* and *P. aeruginosa*. (A) Data are depicted as mean and the error bars represent the standard deviation of triplicates. The plus symbol denotes the classification of biofilms – weak biofilm producer (+), moderate biofilm producer (++), and strong biofilm producer (+++). The asterisks (*) indicate the significant differences between the incubation temperatures ($p < 0.05$). (B) The intensity of CV in wells which corresponds to the incubation temperatures.

Despite the opposing trends observed in the biofilm formation by *S. aureus* and *P. aeruginosa* based on the temperatures, both bacteria were strong biofilm producers at 37°C. Thus, 37°C was selected as the optimum incubation temperature.

To conclude, after the biofilm formation optimizations, the bacterial cells would be prepared in TSB supplemented with 1.0% glucose at 10^8 CFU/mL and incubated at 37°C for the subsequent study.

56

4.2   Purification of Recombinant Endolysin

The SDS-PAGE of the purified recombinant his-tagged endolysin with a molecular weight of 18 kDa is shown in Figure 4.4. The purity of the purified recombinant endolysin was above 95%. The amount of purified recombinant endolysin yield from a 3 L culture was 1.55 mg.
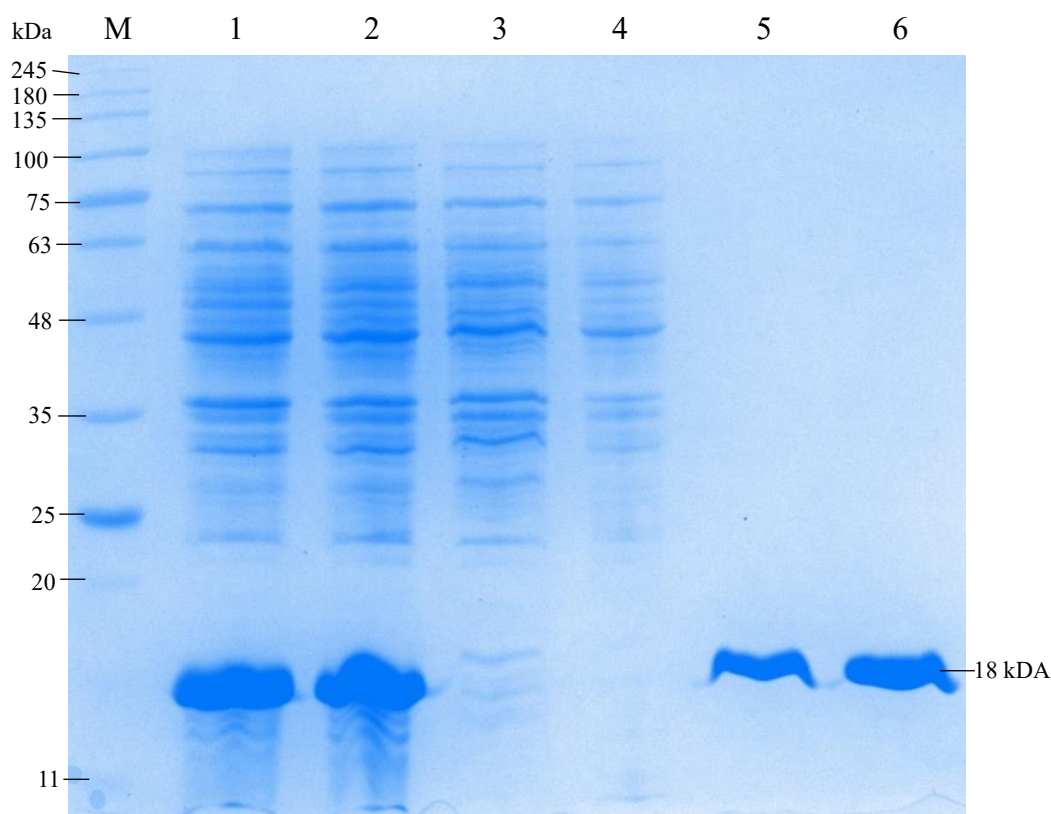
Figure 4.4: Sodium dodecyl sulfate-polyacrylamide gel electrophoresis (SDS-PAGE) analysis of pooled protein samples. M is protein ladder. Lane 1 is the unclarified protein. Lane 2 is clarified protein. Lane 3 is flow-through sample. Lane 4 is wash sample. Lane 5 is the purified recombinant endolysin. Lane 6 is the pooled recombinant endolysin purified samples.

4.3 Biofilm Inhibitory Activity of The Purified Recombinant Endolysin.

4.3.1 Inhibitory Effect of Recombinant Endolysin on *S. aureus* Biofilm Formation

Based on the mean absorbance values in Figure 4.5(A), lower amounts of recombinant endolysins ranging from 0.098 – 1.563 µg significantly reduced (p < 0.05) the biofilm formation by *S. aureus* compared to the control. About 50% of the biofilm mass formation was inhibited with 0.195 – 0.781 µg of recombinant endolysins, as shown in Figure 4.6, which was in parallel with the lowest CV intensity seen in wells number 3 and 5 (Figure 4.5(B)). Based on the results, the highest inhibition obtained was 50%. When higher amounts of endolysin (6.25 – 100 µg) were used, the mass of biofilm produced by *S. aureus* was higher than the control, as seen by the higher mean absorbance values in Figure 4.5(A). Thus, there was no inhibitory activity at these amounts of endolysin, as depicted in Figure 4.6.
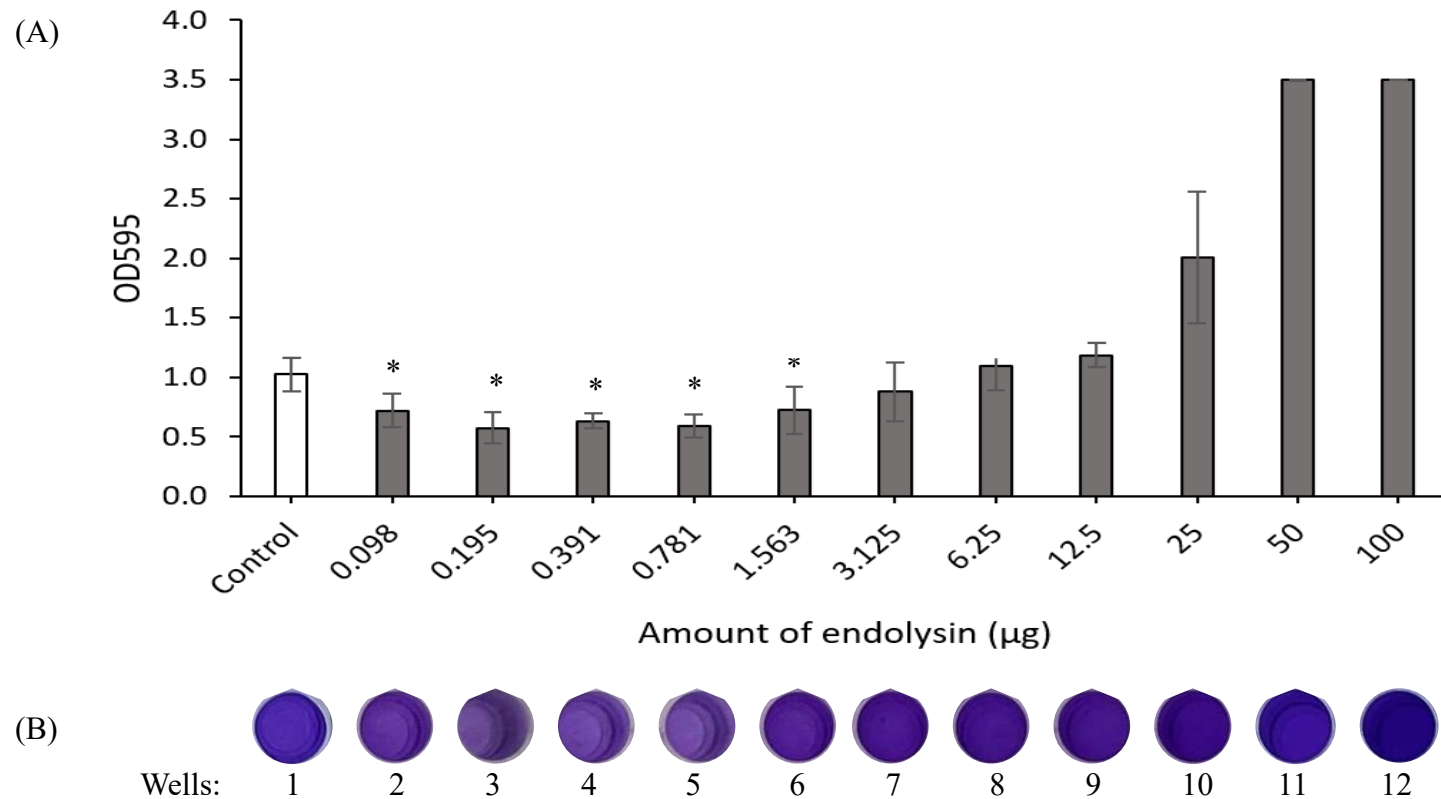
Figure 4.5: Biofilm inhibition activity of recombinant endolysin against forming biofilm of *S. aureus*. *Staphylococcus aureus* was treated with different amounts of recombinant endolysins for 24 h. Control: bacterial cells only. (A) Data are depicted as mean and the error bars refer to the standard deviation of triplicates. The asterisks (*) indicate the significant differences between treatments and control ($p < 0.05$). (B) The CV intensity in each well which corresponds to the amount of endolysin.

Figure 4.6: Percentage of biofilm inhibition by different amounts of recombinant endolysin against forming biofilm of *S. aureus*. Data are presented as mean and the error bars represent the standard deviation of triplicates.

4.3.2 Inhibitory Effect of Recombinant Endolysin on *P. aeruginosa* Biofilm Formation

Pseudomonas aeruginosa is a Gram-negative bacterium, hence, it requires a chelating agent, ethylenediaminetetraacetic acid (EDTA), to increase the permeability of the outer membrane towards endolysins. The treatment with 5 mM EDTA without the endolysins did not show a significant difference from the control without EDTA and endolysins ($p > 0.05$), as shown in Figure 4.7(A). This indicates that EDTA did not interfere with the biofilm inhibitory activity of endolysin.

Treatments with lower amounts of endolysin (0.098 - 3.125 µg) significantly inhibited the biofilm formation compared to the control ($p < 0.05$). Based on the mean absorbance values, a decreasing trend in the biofilm mass formation was observed when the amounts of endolysin increased from 0.098 to 0.781 µg (Figure 4.7(A)). However, no inhibition on the biofilm formation was observed when *P. aeruginosa* was treated with higher amounts of endolysin (6.25 – 100 µg).

Based on the percentage of biofilm inhibition, the lowest amount of endolysin at 0.098 µg was able to inhibit 50% of the biofilm formed by *P. aeruginosa* (Figure 4.8). When the endolysin was increased to 0.781 µg, 81% of the biofilm formation was inhibited, as shown in Figure 4.8. This is further supported by the low CV staining intensity in well number 6 in comparison to other concentrations (wells number 3-5), as shown in Figure 4.7(B). However, the percentage of inhibition dropped when the amount of endolysins further increased to more than 0.781 µg.
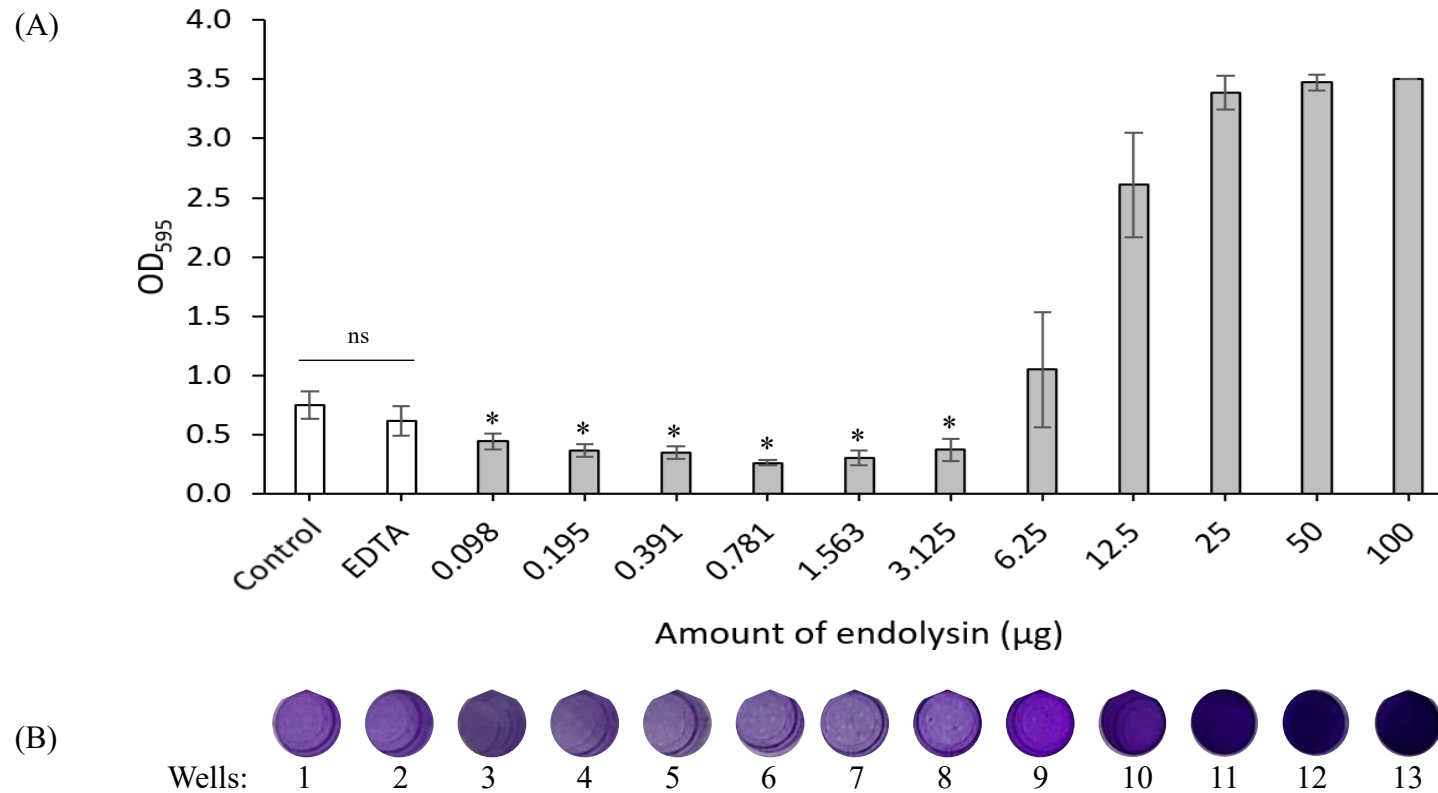
Figure 4.7: Biofilm inhibition activity of recombinant endolysin against forming biofilm of *P. aeruginosa*. *Pseudomonas aeruginosa* were treated with different amounts of recombinant endolysins and 5 mM EDTA for 24 h. Control: bacterial cells only. EDTA: contained bacterial cells with 5 mM EDTA in the absence of endolysin. (A) Data are depicted as mean and the error bars refer to the standard deviation of triplicates. The asterisks (*) indicate the significant differences between treatments and control ($p < 0.05$). "ns" represents no significant difference between control and EDTA. (B) CV staining intensity in each well which corresponds to the amount of endolysin.

Figure 4.8: Percentage of biofilm inhibition by different amounts of recombinant endolysin against forming biofilm of *P. aeruginosa*. Data are shown as mean and the error bars represent the standard deviation of triplicates.

4.4   Biofilm Eradication Activity of Recombinant Endolysin on Biofilm Formation.

4.4.1   Eradication Effect of Recombinant Endolysin on *S. aureus* Mautre Biofilm

Figure 4.9(A) showed a significant drop ($p < 0.05$) in the mean absorbance values of endolysin amount ranging from 0.098 to 3.125 µg compared to the control, indicating that these amount of endolysin could effectively eradicate the mature biofilms produced by *S. aureus*. The lower CV staining intensity from wells number 2 to 7 in comparison to the control in well number 1 further supported the above observation (Figure 4.9(B)).

Based on the percentage of biofilm eradication, it was observed that 1.563 µg endolysin could remove about 50% of the mature biofilm, as illustrated in Figure 4.10. On the other hand, the highest biofilm eradication percentage, 58% was achieved when 0.098 µg endolysin was used to treat the mature biofilm formed by *S. aureus*. On the contrary, the amount of endolysin was increased above 3.125 µg, it showed no eradication activity.
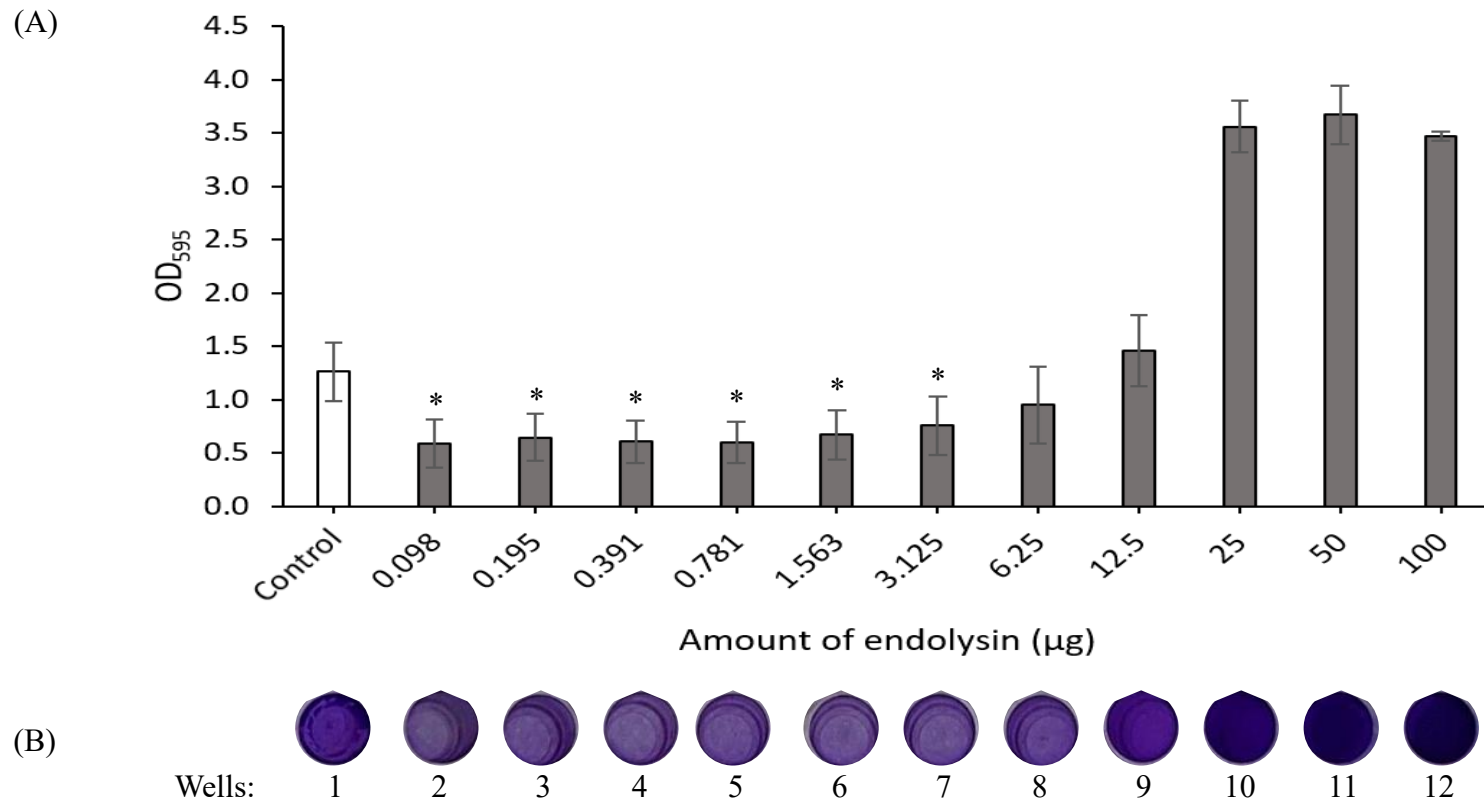
Figure 4.9: Biofilm eradication activity of recombinant endolysin against mature biofilm of *S. aureus*. Biofilms of *S. aureus* were treated with different amounts of recombinant endolysins for 24 h. Control: bacterial cells only. (A) Data are presented as mean and the error bars represent the standard deviation of triplicates. The asterisks (*) indicate the significant differences between treatments and control ($p < 0.05$). (B) CV staining intensity in each well which corresponds to the amount of endolysins.
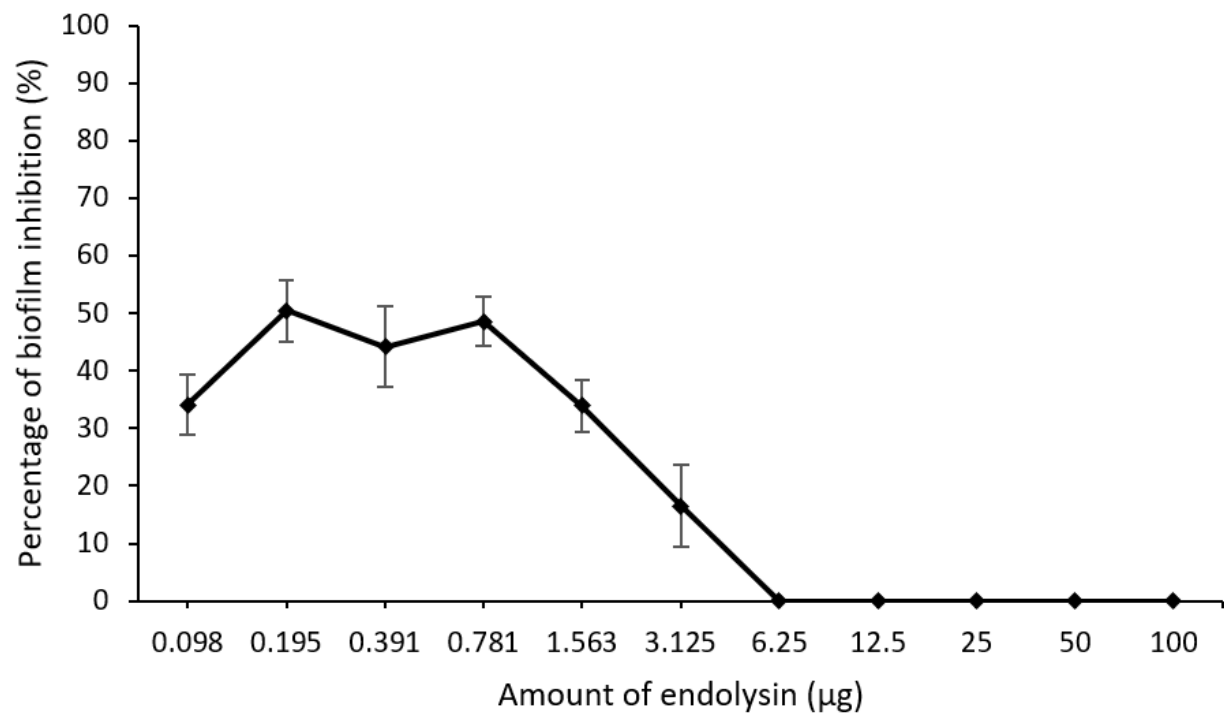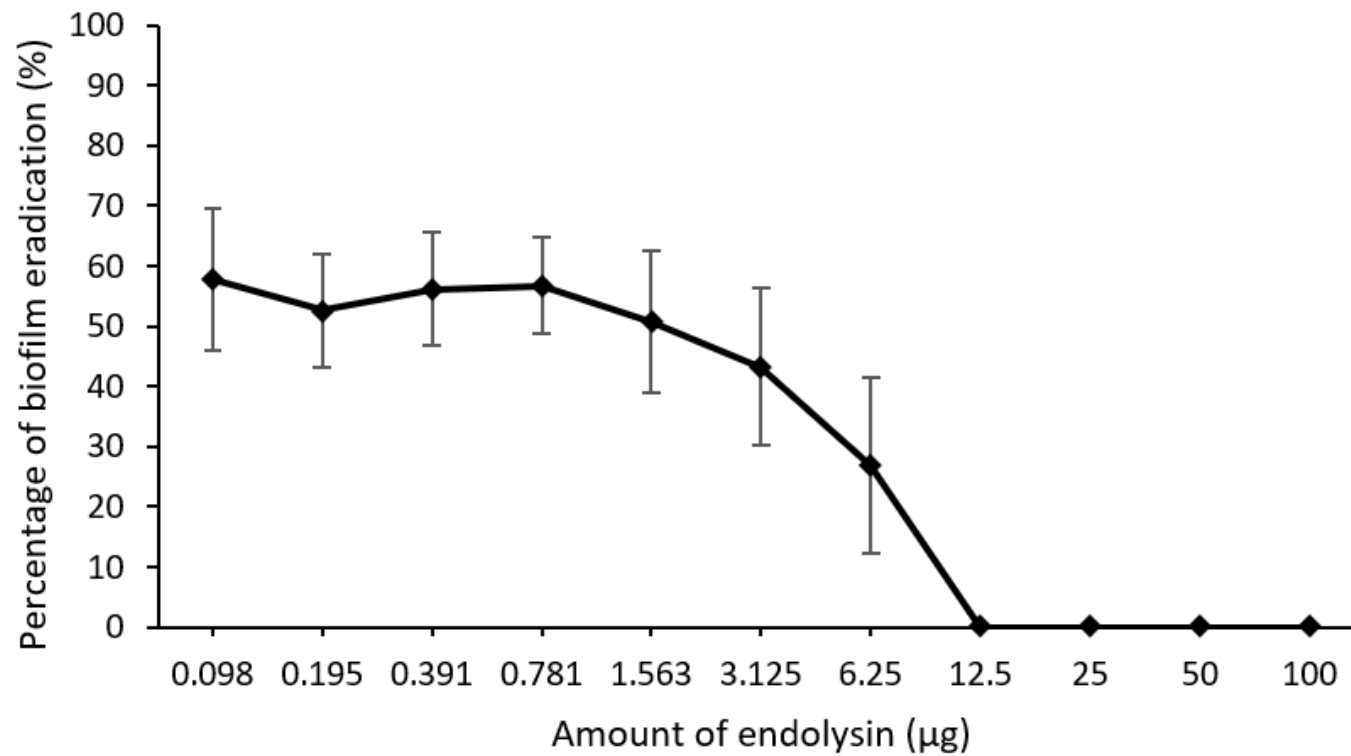
Figure 4.10: Percentage of biofilm eradication by different amounts of recombinant endolysin against mature biofilm of *S. aureus*. Data are depicted as mean and the error bars refer to the standard deviation of triplicates.

4.4.2 Eradication Effect of Recombinant Endolysin on *P. aeruginosa* Mautre Biofilm

Based on the results obtained, 5 mM EDTA treatment did not affect endolysin and the biofilm formed was similar to that observed in the control ($p > 0.05$).

Figure 4.11(A) showed a decrease in the biofilm mass as the endolysin amount increased from 0.098 µg to 0.781 µg, whereby the intensity of CV staining also decreased, as shown in wells 3 to 6 (Figure 4.11(B)). However, the mean absorbance values of the endolysin amount ranging from 0.391 to 3.125 µg significantly drop ($p < 0.05$) as compared to the control, as depicted in Figure 4.11(A). Based on the percentage of biofilm eradication, about 50% of the mature biofilms could be eradicated by 0.195 µg of endolysins. However, 0.391 – 1.563 µg of endolysins could significantly eradicate ($p < 0.05$) about 90% of the mature biofilms. When the amount of endolysin was increased up to 100 µg, an increase in the biofilm mass was observed in Figure 4.11(A).

(A)

(B) Wells: 1 2 3 4 5 6 7 8 9 10 11 12 13
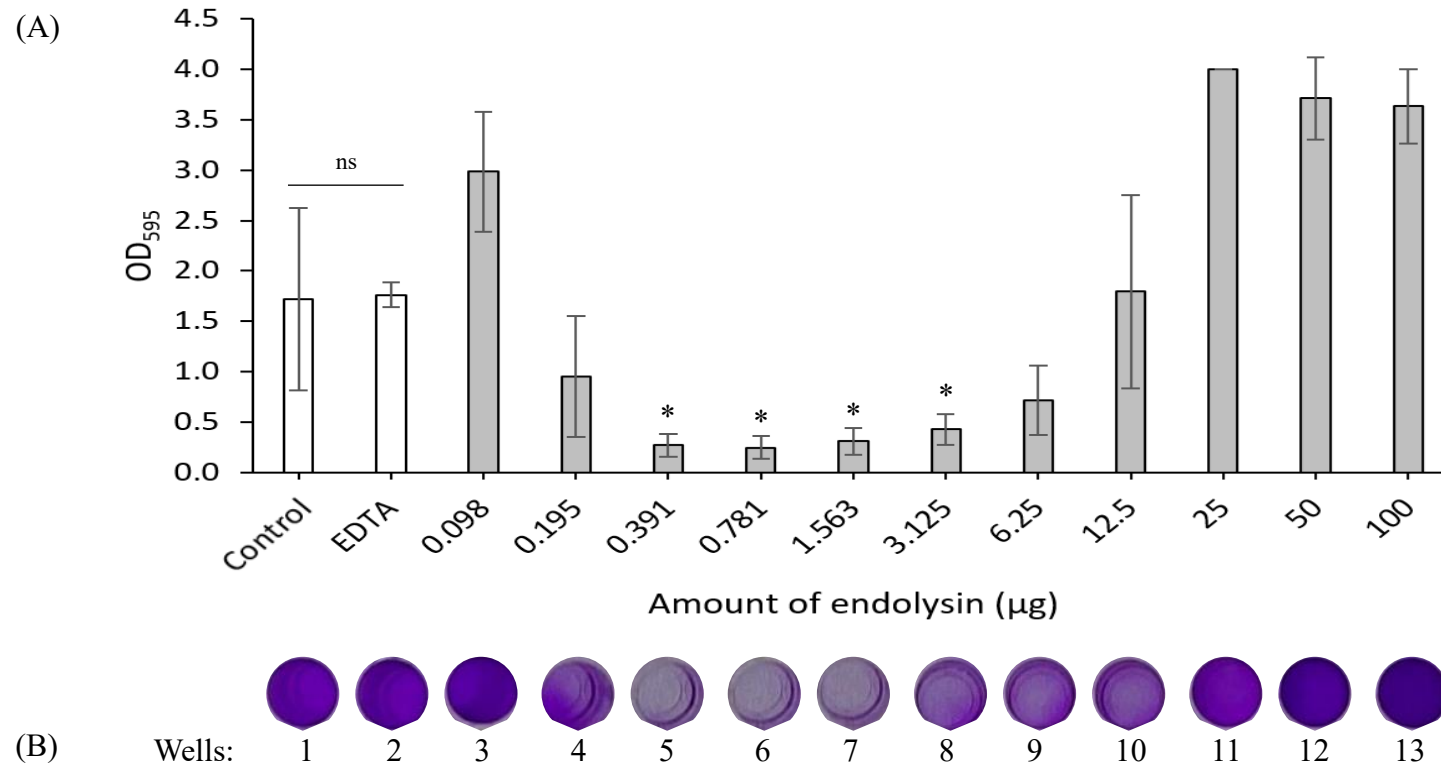
Figure 4.11: Biofilm eradication activity of recombinant endolysin against mature biofilm of *P. aeruginosa*. Biofilms of *P. aeruginosa* were treated with different amounts of recombinant endolysins and 5 mM EDTA for 24 h. Control: bacterial cells only. EDTA: contained bacterial cells with 5 mM EDTA in the absence of endolysin. (A) Data are expressed as mean and the error bars represent the standard deviation of triplicates. The asterisks (*) indicate the significant differences between treatments and control ($p < 0.05$). "ns" denotes no significant difference between control and EDTA. (B) CVstaining intensity in each well which corresponds to the amount of endolysin.

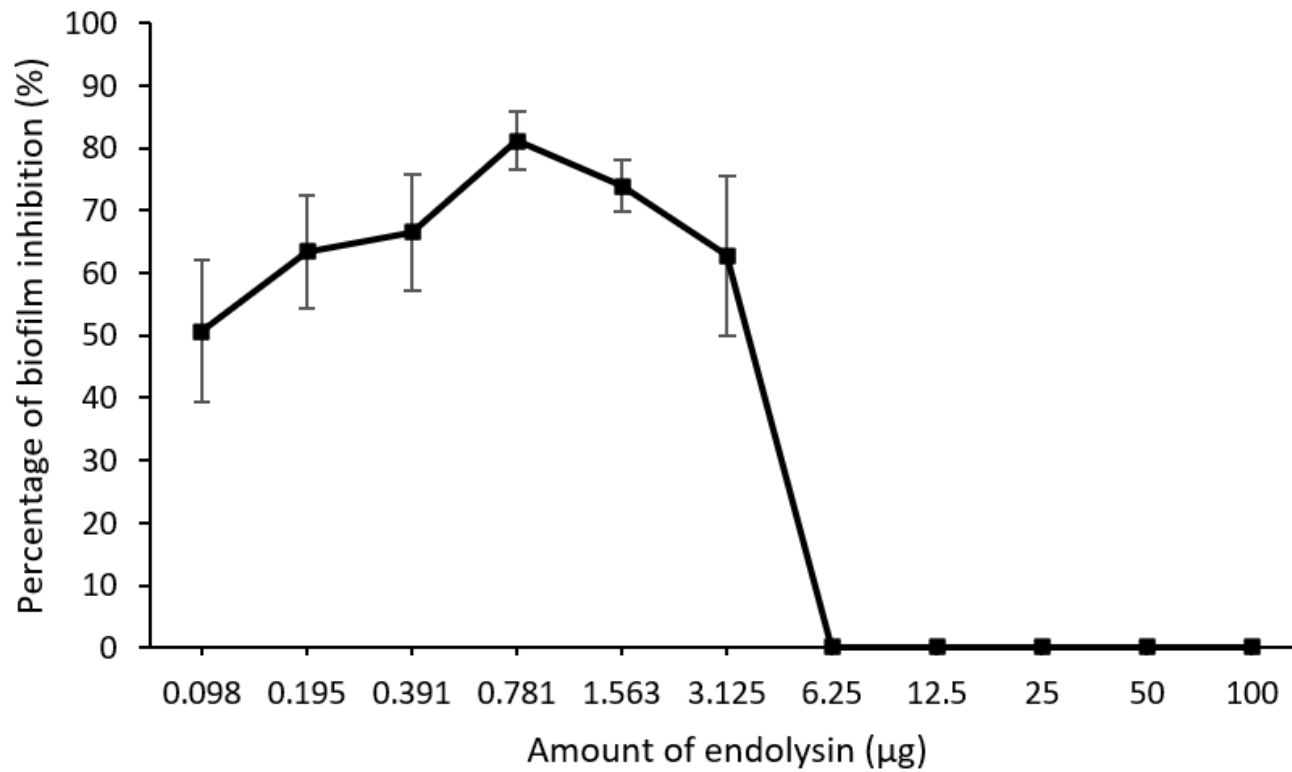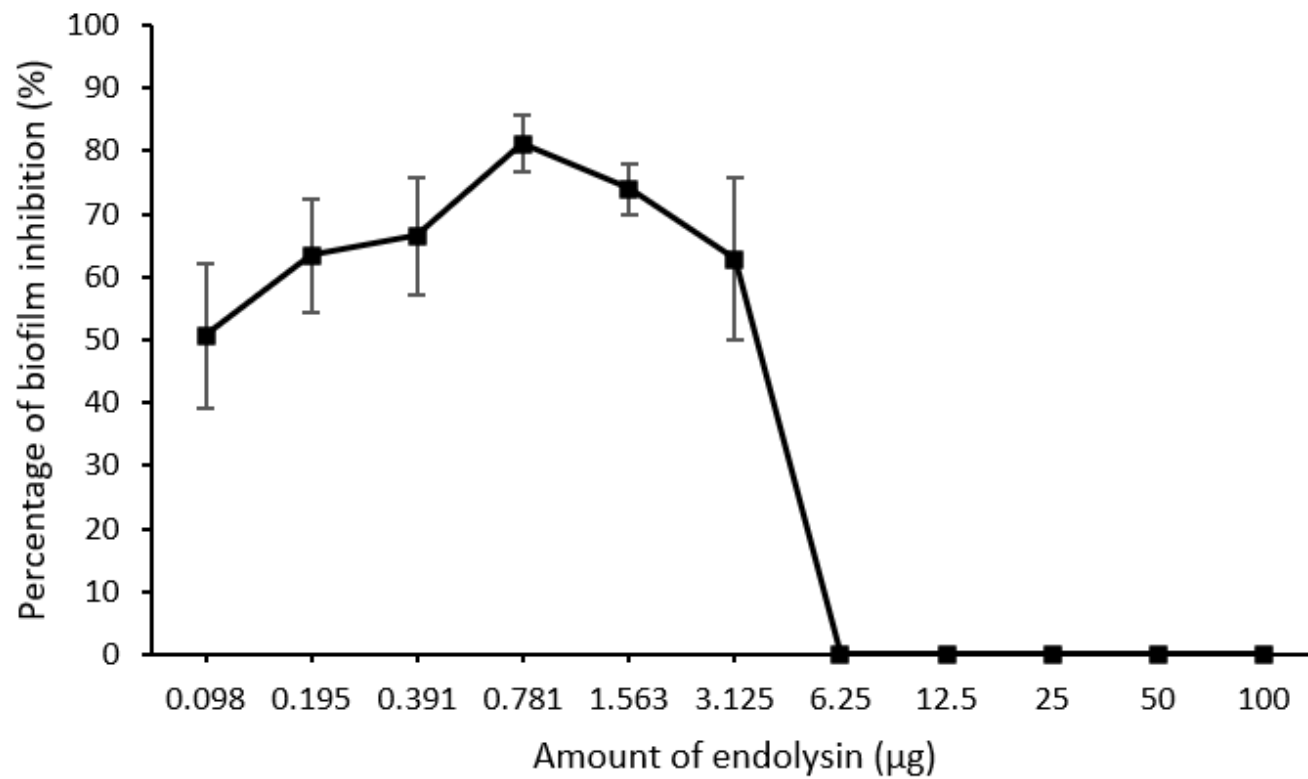**Figure 4.12:** Percentage of biofilm eradication by different amounts of recombinant endolysin against mature biofilm of *P. aeruginosa*. Data are expressed as mean and the error bars refer to the standard deviation of triplicates.

CHAPTER 5

DISCUSSION

Biofilms-associated multidrug resistance (MDR) is a rising issue in the medical field which leads to increasing rates of patients' morbidity and mortality (Assefa and Amare, 2022). *Staphylococcus aureus* and *Pseudomonas aeruginosa* are two of the most predominant bacteria that result in the biofilm associated MDR in healthcare associated infection (Zhao, Sun and Liu, 2023). The treatment for these bacterial infections has become more challenging as the antibiotic treatments are no longer effective. As a result, novel antimicrobial agents are continuously being discovered. Thus, biofilms related studies involving the novel antibiofilm agents have become very essential. Recombinant phage endolysins have been shown to be an ideal antibacterial agent in combating these biofilms-associated MDR bacterial cells (Rahman, et al., 2021).

5.1 Optimization of Biofilm Formation

Optimization of biofilm formation prior to the evaluation of any antibiofilm agent is essential to achieve clinically significant antibiofilm assays (Lade, et al., 2019; Thieme, et al., 2019).

5.1.1 Effect of Glucose Concentration on Biofilm Formation

Different parameters have been investigated and different growth media have been studied. So far, tryptic soy broth (TSB) has been commonly used as the medium for biofilm growth (Cha, Son and Ryu, 2019; Miao, et al., 2019; Zhang,

et al., 2022; Soontarach, et al., 2024). Apart from that, supplementation of growth medium with glucose has also been used to promote biofilm growth.

In this study, biofilm formation by *S. aureus* was directly proportional to the glucose concentration. Similarly, a study has reported that the biofilm mass produced by *S. aureus* increased when glucose concentrations of 0.25% and 1.0% were used (Sar and Akbas, 2019). Moreover, in another study, clinically isolated *S. aureus* showed high biofilm mass formation with glucose concentration up to 1.0% (Lade, et al., 2019).

When *S. aureus* is grown in culture medium supplemented with glucose, fermentation will occur, which in turn decrease the pH of the medium by acid byproducts (Luo, et al., 2020; Matilla-Cuenca, et al., 2022). The acidic environment then initiated polymerization of functional amyloids into amyloid-like fibers, which will promote biofilm growth (Lade, et al., 2019; Matilla-Cuenca, et al., 2022). According to Lade, et al. (2019), extracellular protease production could be repressed by acidic pH. This allowed the assembly of functional amyloids which facilitates the biofilm formation by *S. aureus*.

In a study conducted by She et al. (2019), *P. aeruginosa* biofilm formation was enhanced with increasing glucose concentration, which is in accordance with the current findings. An increase in glucose concentration could significantly enhance the expression of *pslA* gene in *P. aeruginosa*. This, in turn, increased the production of extracellular polysaccharides, which play a significant role in the adherence of the biofilm bacterial cells between the cells and the surfaces

(Limoli, Jones and Wozniak, 2015; She, et al., 2019). The adherence to the surface is driven by the synthesis of bis-(3′-5′)-cyclic dimeric guanosine monophosphate (c-di-GMP) through Psl synthesis (Vandana and Das, 2022). Subsequently, c-di-GMP (secondary messenger) drives the production of extracellular polysaccharides production, thus increasing the biofilm mass formation.

5.1.2 Effect of Initial Bacterial Cell Titer on Biofilm Formation

Initial bacterial cell titer also has an impact on the biofilm mass formation. The present study reported that the higher the bacterial cell titer in the initial inoculum, the higher the amount of biofilm mass produced by *S. aureus* and *P. aeruginosa*. A similar finding was reported by Roberts (2016), in which an increasing trend in biofilm production by *P. aeruginosa* was shown with increasing initial bacterial cell titer.

Biofilm formation was initiated by the attachment of bacterial cells to the surface and produce extracellular polymeric substances (EPS) (Cho, Shi and Boost, 2015). EPS further assists in the adherence of the bacterial cells to the surface and provides stability to the biofilm (Pommerville, 2021). Therefore, the higher the initial bacterial cell titer, the higher the number of bacterial cells that would adhere to the surface, hence resulting in a higher amount of EPS, which enhanced biofilm formation.

Besides, biofilm formation is greatly influenced by quorum sensing (Reddersen, et al., 2021). The bacterial cells need to reach a certain quorum before they could sense or communicate with one another through the production of autoinducers (AIs) (Willey, Sandman and Wood, 2020). AIs are signaling molecules that coordinate the bacterial cells towards the formation and growth of the biofilm (Preda and Săndulescu, 2019; Willey, Sandman and Wood, 2020). Thus, it could be inferred that a higher bacterial titer in the initial inoculum achieves a quorum at a faster rate which promotes the synthesis of AIs to facilitate biofilm formation (Cho, Shi, and Boost, 2015).

On the other hand, this study has demonstrated that bacterial suspension containing 10^9 CFU/mL reduced biomass formation. This observation could be due to the limited growth conditions when a higher initial bacterial cell titer was used (Salgar-Chaparro, 2020). For instance, the nutrients in the culture medium would be insufficient for a higher bacterial titer, which led to a decrease in biofilm formation (Salgar-Chaparro, 2020).

5.1.3 Effect of Incubation Temperature on Biofilm Formation

Temperature also has a major impact on biofilm growth because temperature can influence the bacterial growth and metabolism, and production of EPS (Alotaibi and Bukhari, 2021). *Staphylococcus aureus* and *P. aeruginosa* showed a different growth behavior with incubation temperatures, as observed in this study. The increasing temperature has resulted in the increased biofilm mass formation by *S. aureus* similar to that reported by Miao, et al. (2019), where 37°C was the optimum temperature to use for the highest biofilm mass formation.

At a higher temperature, the metabolic activity of the bacterial cells increases which accelerates their growth and production of EPS (Willey, Sandman and Wood, 2020; Pommerville, 2021). Thus, this could facilitate the biofilm formation by *S. aureus* compared to lower temperatures, as shown in this study.

On the other hand, the production of biofilm by different *P. aeruginosa* clinical isolates varies with different incubation temperature (Al-Khazraji and Al-Maeni, 2021). However, most of the clinical strains produced higher biofilm mass at 25°C, compared to 37°C, which is parallel to the present study (Al-Khazraji and Al-Maeni, 2021). In addition, another *P. aeruginosa* strain, PA14 exhibited a decreased biofilm mass as the temperature increased from 20 to 37°C, which further supports the findings in this study (Kim, et al., 2020b).

A previous study has shown that this phenomenon could be due to the expression of *pelA* gene, and synthesis of c-di-GMP and exopolysaccharide which were relatively reduced at higher temperatures (Kim, et al. 2020b). As the temperature decreases, the metabolic activity of *P. aeruginosa* also changes. Therefore, the c-di-GMP synthesis would increase, inducing the production of more exopolysaccharides that mediates biofilm formation (She, et al., 2019; Kim, et al., 2020b).

5.2 Antibiofilm Activity of Recombinant Endolysin Against *S. aureus* and *P. aeruginosa*

Staphylococcus aureus and *P. aeruginosa* are MDR bacteria in nature (Ryan, 2022). The ability to form biofilms further enhances their resistance towards antibiotics. This has led to increased cases of biofilm-associated infections, which are more difficult to treat with antibiotics (Pachori, Gothalwal and Gandhi, 2019).

Recombinant endolysins are single proteins that show rapid antibiofilm activities with a lower risk of immunological response and resistance development (Yang, et al., 2020; Rahman, et al., 2021). This makes endolysin a promising antibiofilm agent.

Many studies have shown that exogenous administration of endolysins could effectively penetrate the biofilm and lyse the individual cells by degrading their cell walls (Fursov, et al., 2020; Lu, et al., 2021; Ning, et al., 2021; Rahman, et al., 2021). As biofilm embedded cells are lysed, the biofilm will be destabilized and detached from the surface. Hence, recombinant endolysins could effectively inhibit biofilm formation or eradicate the mature biofilm.

5.2.1 Inhibitory Effect of Recombinant Endolysin on Biofilm Formation by *S. aureus* and *P. aeruginosa*

In this study, the recombinant endolysin showed inhibitory activity against the formation of biofilm by both *S. aureus* and *P. aeruginosa*. The recombinant endolysin in the current study could inhibit 50% of biofilms produced by *S. aureus* at 1.95 μg/mL (0.195 μg). In one study, about 50% of the biofilm was

inhibited by LysAB1245 endolysin with a concentration of 1.17 μg/mL, which was lower than the endolysin concentration used in the present study (Soontarach, et al., 2024). Furthermore, in a previous study, 0.59 μg/mL of LysAB1245 was sufficient to inhibit about 50% of the biofilm formation by *P. aeruginosa*. This concentration is also lower than the concentration of endolysin used in this study to achieve a similar result (Soontarach, et al., 2024).

The difference in the efficiency of these endolysins could be due to their different host range. The current endolysin and LysAB1245 were derived from gram-negative bacteria targeting phages, Escherichia phage and A. baumannii phage T1245, respectively (Soontarach, et al., 2024). Different origins of the endolysins lead to variations in their catalytic domains, which are responsible for their specificities and efficacies (Liu, et al., 2023; Soontarach, et al., 2024).

Besides, endolysins have been engineered to enhance further their antibacterial and antibiofilm activity (Son, et al., 2020; Gutiérrez, et al., 2021). Previous findings reported that the engineered LysRODIΔAmi endolysin could effectively inhibit 90% of the biofilm formation by *S. aureus* with a minimum concentration of 0.15 μM, which was proven to be more effective compared to the current unmodified endolysins (Gutiérrez, et al., 2021). The engineered endolysins were produced by fusing the cell-wall binding domains and the catalytic domains from different endolysins which resulted in increased specificity of the engineered endolysins (Son, et al., 2020; Gutiérrez, et al., 2021). This would in turn enhance the efficacy of the engineered endolysins.

On the other hand, no inhibition of biofilm formation was observed at a higher amount of endolysin against *S. aureus* and *P. aeruginosa* in the present study. This observation could be due to increased stress generated by the higher amount of endolysin which activated the stress response in the bacteria (Mitchell and Silhavy, 2019; Dawan and Ahn, 2022). The excessive peptidoglycan disruption by the high amount of endolysin activated the stress response. As a result, the peptidoglycan synthesis would be modified with a higher number of crosslinking and the expression of genes responsible for biofilm could be activated, increasing biomass formation and inactivating the endolysin (Mitchell and Silhavy, 2019).

5.2.2 Eradication Effect of Recombinant Endolysin on Mature Biofilm Formed by *S. aureus* and *P. aeruginosa*

The biofilm eradication activity of the endolysin is crucial because biofilm could further enhances the resistance to antibiotics (Rahman, et al., 2021). Current study showed that the recombinant endolysin could significantly remove the mature biofilms produced by *S. aureus* and *P. aeruginosa*. A total of 50% of *S. aureus* biofilm was eradicated with 15.63 µg/mL of endolysins for 24 h in this study.

In one study, the removal of 50% of *S. aureus* biofilm was reported with 18.72 µg/mL of LysAB1245, derived from *Acinetobacter* phage T1245, for 24 h (Soontarach, et al., 2024). This showed that the recombinant endolysin in this study was more effective in eradicating *S. aureus* biofilm than LysAB1245. Moreover, Lu, et al. (2021) reported that a higher concentration of LysP108, derived from *Staphylococcus* phage P108, was needed to eradicate more biofilm

produced by *S. aureus* compared to the current endolysin. The difference in the efficiency between the previous endolysins and current endolysin could be due to the different strains of *S. aureus* (Sharma, et al., 2023). This is because the peptidoglycan subunits may be different from each strain, which could influence the catalytic activity of endolysins (Rohde, 2019; Liu, et al., 2023).

On the contrary, another endolysin, LysCSA13, was more effective in eliminating the mature biofilm of *S. aureus* than the current endolysin where 8.51 μg/mL of LysCSA13 eradicated 90% of the biofilm within an hour (Cha, Son and Ryu, 2019). LysCSA13, which originated from S. aureus bacteriophage CSA13, was more effective than the current endolysin could be attributed to the cell-wall binding domain (CBD) in LysCSA13 (Cha, Son and Ryu, 2019). The CBD of LysCSA13 is more specific to *S. aureus* compared to the current endolysin, which lacks the CBD, and thus, this could contribute to higher eradication activity of LysCSA13 against *S. aureus* biofilm.

On the other hand, a near complete elimination (93%) of *P. aeruginosa* biofilm within 24 h was achieved with 0.781 μg in the current study. In contrast, a higher amount (3.744 μg) of LysAB1245, derived from Acinetobacter phage T1245, was required to eradicate up to 94% of the biofilm formed by *P. aeruginosa* in 24 h (Soontarach, et al., 2024). Besides, LysSTG2 from Salmonella-lytic bacteriophage STG2 and LysPA26 from P. aeruginosa phage JD010 required up to 200 μg and 100 μg to remove about 50% of the mature biofilm produced by *P. aeruginosa* (Guo, et al., 2017; Zhang, et al, 2022). This showed that the concentrations of LysSTG2 and LysPA26 required for biofilm eradication were

significantly higher than the concentration of present endolysins. Therefore, the endolysin in this study was more efficient in eradicating the biofilms formed by *P. aeruginosa* compared to LysAB1245, LysSTG2 and LysPA26.

The above phenomenon could be due to the target specificity of the endolysins (Liu, et al., 2023). The endolysins would show a higher antibiofilm activity against its target-specific bacteria but lesser activity against other bacteria (Liu, et al., 2023). For instance, 200 μg LysSTG2 could only remove about 50% of *P. aeruginosa* biofilm but removed 99.99% of *P. putida* biofilm (Zhang, et al, 2022). Therefore, this showed that LysSTG2 was more specific towards *P. putida*. Similarly, the current endolysin which may be more specific to *P. aeruginosa* compared to the previous endolysins and hence, the current endolysin showed a higher biofilm eradication efficiency.

5.3   Limitations

One of the limitations was that the viability test, which complements the crystal violet (CV) staining, was not carried out, and thus, the dead cells that remained in the biofilm were not identified. This is because CV staining could not assess the killing of biofilm cells as both live and dead bacteria could take the CV stain up (Yang, et al., 2020). In this study, the efficacy of the recombinant endolysin as an antibiofilm agent was evaluated. However, the actual mechanism of action on how the recombinant endolysins inhibit and eradicate the biofilm was not fully understood.

5.4   Future Recommendations

In future studies, the viability test should be included as part of the evaluation of antibiofilm assays. Visualization using a scanning electron microscope (SEM) could further enhance the evaluation quality of the antibiofilm assays. Moreover, further studies should be conducted to investigate the absence of biofilm inhibition and eradication activity with a higher amount of endolysin used. on the interactions between endolysins and the biofilm have to be carried out to understand the endolysin mechanism of action. Besides, studies on the interactions between endolysin and biofilm should be carried out to understand the biofilm inhibition and eradication mechanisms of endolysin. This study could be repeated with clinical strains to study the antibiofilm activity of endolysins against clinical strains.

CHAPTER 6

CONCLUSION

In conclusion, this study has demonstrated that both *Staphylococcus aureus* and *Pseudomonas aeruginosa* are strong biofilm producers when a bacterial cell titer of 10^8 CFU/mL was used as the initial inoculum and cultured in TSB supplemented with 1.0% glucose at 37°C.

The recombinant endolysin has exhibited an effective antibiofilm effect against the biofilms formed by both bacteria. The minimum 50% biofilm inhibition concentrations ($MBIC_{50}$) against *S. aureus* and *P. aeruginosa* were determined at 1.95 – 7.81 µg/mL and 0.98 µg/mL, respectively. However, the minimum 90% biofilm inhibition concentration ($MBIC_{90}$) could not be achieved.

On the other hand, the minimum 50% biofilm eradication concentration ($MBEC_{50}$) was achieved against *S. aureus* and *P. aeruginosa* at 15.63 – 31.25 µg/mL and 1.95 µg/mL, respectively. The minimum 90% biofilm eradication concentration ($MBEC_{90}$) was only achieved against *P. aeruginosa* at 3.91 – 15.63 µg/mL.

Therefore, this study has demonstrated that recombinant endolysin can be a potential antibiofilm agent. Further investigation can be performed to evaluate the endolysin as antibiofilm agent against clinical strains.

REFERENCES

Abdelrahman, F., Easwaran, M., Daramola, O.I., Ragab, S., Lynch, S., Oduselu, T.J., Khan, F.M., Ayobami, A., Adnan, F., Torrents, E., Sanmukh, S. and El-Shibiny, A., 2021. Phage-encoded endolysins. *Antibiotics*, *10*(2), p.124.

Agrawal, A.A., Pawar, K.A., Gegade, V.N., Kapse, A.A. and Patravale,V.B., 2022. Nanobiomaterials for medical devices and implants. In: H.H. Liu, T. Shokuhfar and S. Ghosh, eds. 2022. *Nanotechnology in medicine and biology*. Amsterdam: Elsevier. pp.235-272.

Al-Khazraji, S.F.R. and Al-Maeni, M.A.R., 2021. Optimization of some environmental and nutritional conditions using microtiter plate for *Pseudomonas aeruginosa* biofilm formation. *Journal of Animal Behaviour and Biometeorology*, 9(4), pp.2136.

Alotaibi, G.F. and Bukhari, M.A., 2021. Factors influencing bacterial biofilm formation and development. *American Journal of Biomedical Science & Research*, 12(6), pp.617-626.

Assefa, M. and Amare, A., 2022. Biofilm-associated multi-drug resistance in hospital-acquired infections: a review. *Infection and Drug Resistance*, 15, pp.5061-5068.

Bamford, N.C., MacPhee, C.E. and Stanley-Wall, N.R., 2023. Microbial primer: an introduction to biofilms - what they are, why they form and their impact on built and natural environments. *Microbiology*, 169(8), p.001338.

Barron, M, 2022. *Phage therapy: past, present and future*. [online] Available at: < https://asm.org/articles/2022/august/phage-therapy-past,-present-and-future> [Accessed 14 January 2024].

Becker, S.C., Swift, S., Korobova, O., Schischkova, N., Kopylov, P., Donovan, D.M. and Abaev, I., 2015. Lytic activity of the staphylolytic Twort phage endolysin CHAP domain is enhanced by the SH3b cell wall binding domain. *FEMS Microbiology Letters*, 362(1), pp.1-8.

Cangui-Panchi, S.P., Ñacato-Toapanta, A.L., Enríquez-Martínez, L.J., Salinas-Delgado, G.A., Reyes, J., Garzon-Chavez, D. and Machado, A., 2023. Battle royale: Immune response on biofilms – host-pathogen interactions. *Current Research in Immunology*, 4, p.100057.

Cernooka, E., Rummieks, J., Zrelovs, N., Tars, K. and Kazaks, A., 2022. Diversity of the lysozyme fold: structure of the catalytic domain from an unusual endolysin encoded by phage Enc34. *Scientific Reports*, 12, p.1-11.

Chamblee, J.S., Ramsey, J., Chen, Y., Maddox, L.T., Ross, C., To, K.H., Cahill, J.L. and Young, R., 2022. Endolysin regulation in Phage Mu lysis. *American Society for Microbiology*, 13(3), p.e0081322.

Cha, Y., Son, B. and Ryu, S., 2019. Effective removal of staphylococcal biofilms on various food contact surfaces by *Staphylococcus aureus* phage endolysin LysCSA13. *Food Microbiology*, 84, p.103245.

Cho, P., Shi, G.S. and Boost, M., 2015. Inhibitory effects of 2,2′-dipyridyl and 1,2,3,4,6-penta-o-galloyl-b-d-glucopyranose on biofilm formation in contact lens cases. *Investigative Ophthalmology and Visual Science November*, 56(12), pp.7053-7057.

Cong, Y., Yang, S. and Rao, X., 2019. Vancomycin resistant *Staphylococcus aureus* infection: A review of case updating and clinical features. *Journal of Advanced Research*, 21(2020), pp.169-176.

Dashtbani-Roozbehani, A. and Brown, M.H., 2021. Efflux pump mediated antimicrobial resistance by staphylococci in health-related environments: challenges and the quest for inhibtion. *Antibiotics*, 10(12), p.1502.

Dawan, J. and Ahn, J., 2022. Bacterial stress responses as potential targets in overcoming antibiotic resistance. *Microorganisms*, 10(7), p.1385.

Di Martino, P., 2018. Extracellular polymeric substances, a key element in understanding biofilm phenotype. *AIMS Microbilogy*, 4(2), pp.274-288.

Ellen, M., Draper, L.A., Ross, R.P. and Hill, C., 2021. The advantages and challenges of using endolysins in a clinical setting. *Viruses*, 13(4), p.680.

Extremina, C.I., Costa, L., Aguiar, A.I., Peixe, L. and Fonseca, A.P., 2011. Optimization of processing conditions for the quantification of enterococci biofilms using microtiter-plates. *Journal of Microbiological Methods*, 84(2), pp.167-173.

Fakhro, A., Jalalabadi, F., Brown, R.H. and Izaddoost, S.A., 2016. Treatment of infected cardiac implantable electronic devices. *Seminars in Plastic Surgery*, 30(2), pp.60–65.

Fan, Y. and Pedersen, O., 2021. Gut microbiota in human metabolic health and disease. *Nature Reviews Microbiology*, 19(1), p.55.

Fursov, M.V., Abdrakhmanova, R.O., Antonova, N.P., Vasina, D.V., Kolchanova, A.D., Bashkina, O.A., Rubalsky, O.V., Samotrueva, M.A., Potapov, V.D., Makarov, V.V., Yudin, S.M., Gintsburg, A.L., Tkachuk, A.P., Gushchin, V.A. and Rubalskii, E.O., 2020. Antibiofilm activity of a broad-range recombinant endolysin LysECD7: in vitro and in vivo study. *Viruses*, 12(5), p.545.

Galié, S., García-Gutiérrez, C., Miguélez, E.M., Villar, C.J. and Lombó, F., 2018. Biofilms in the food industry: health aspects and control methods. *Frontiers in Microbiology*, 9, p.898.

Goncalves, A.S.C., Leitao, M.M., Simoes, M. and Borges, A., 2023. The action of phytochemicals in biofilm control. *Natural Product Reports*, 40(3), pp.595-627.

Goodarzi, F., Hallajzadeh, M., Sholeh, M., Talebi, M., Pirhajati Mahabadi, V. and Amirmozafari, N., 2022. Anti-biofilm activity of a lytic phage against vancomycin-resistant *Enterococcus faecalis*. *Iranian Journal of Pathology*, 17(3), pp.285-293.

Guo, M., Feng, C., Ren, J., Zhuang, X., Zhang, Y., Zhu, Y., Dong, K., He, P., Guo, X. and Qin, J., 2017. A novel antimicrobial endolysin, LysPA26, against *Pseudomonas aeruginosa*. *Frontiers in Microbiology*, 8(293).

Guo, Y., Chen, P., Lin, Z. and Wang, T., 2019. Characterization of two *Pseudomonas aeruginosa* viruses vB_PaeM_SCUT-S1 and vB_PaeM_SCUT-S2. *Viruses*, 11(4), p.318.

Gutiérrez, D., Rodríguez-Rubio, L., Ruas-Madiedo, P., Fernández, L., Campelo, A.B., Briers, Y., Nielsen, M.W., Pedersen, K., Lavigne, R., García, P. and Rodríguez, A., 2021. Design and selection of engineered lytic proteins with *Staphylococcus aureus* decolonizing activity. *Frontiers in Microbiology*, 12, (723834).

Guzmán, E., Ortega, F. and Rubio, R.G., 2024. Exploring the world of rhamnolipids: a critical review of their production, interfacial properties, and potential application. *Current Opinion in Colloid & Interface Science*, 69, p.101780.

Haney, E.F., Trimble, M.J. and Hancock, R.E.W., 2021. Microtiter plate assays to assess antibiofilm activity against bacteria. *Nature Protocols*, 16(5), pp.2615-2632.

Hollmann, B., Perkins, M. and Walsh, D., 2018. *Biofilms and their role in pathogenesis*. [online] Available at: <https://www.immunology.org/public-information/bitesized-immunology/pathogens-disease/biofilms-and-their-role-pathogenesis> [Accessed 17 February 2024].

Hong, S., Son, B., Ryu, S. and Ha, N.C., 2019. Crystal structure of LysB4, an endolysin from *Bacillus cereus*-targeting Bacteriophage B4. *Molecules and Cells*, 42(1), pp.79–86.

Iacob, S., Iacob, D.G. and Luminos, L.M., 2019. Intestinal Microbiota as a Host Defense Mechanism to Infectious Threats. *Frontiers in Microbiology*, 9.

Islam, O.K., Islam, I., Saha, O., Rahaman, M.M., Sultana, M., Bockmühl, D.P. and Hossain, M.A., 2023. Genomic variability correlates with biofilm phenotypes in multidrug resistant clinical isolates of Pseudomonas aeruginosa. *Scientific Reports*, 13(1), p.7867.

Khatoon, Z., McTiernan, C.D., Suuronen, E.J., Mah, T.F. and Alarcon, E.I., 2018. Bacterial biofilm formation on implantable devices and approaches to its treatment and prevention. *Heliyon*, 4(12), p.e01067.

Kim, S., Kim, S.H., Rahman, M. and Kim, J., 2018. Characterization of a Salmonella Enteritidis bacteriophage showing broad lytic activity against gram-negative enteric bacteria §. *The Journal of Microbiology*, 56(12), pp.917-925.

Kim, S., Lee, D.W., Jin, J.S. and Kim, J., 2020a. Antimicrobial activity of LysSS, a novel phage endolysin, against *Acinetobacter baumannii* and *Pseudomonas aeruginosa*. *Journal of Global Antimicrobial Resistance*, 22, pp.32-39.

Kim, S., Li, X.H., Hwang, H.J. and Lee, J.H., 2020b. Thermoregulation of *Pseudomonas aeruginosa* biofilm formation. *Applied and environmental microbiology*, 86(22), p.e01584-20.

Lade, H., Park, J.H., Chung, S.H., Kim, I.H., Kim, J.M, Joo, H.S. and Kim, J.S., 2019. Biofilm formation by *Staphylococcus aureus* clinical isolates is differentially affected by glucose and sodium chloride supplemented culture media. *Journal of Clinical Medicine*, 8(11), p.1853.

Limoli, D.H., Jones, C.J. and Wozniak, D.J., 2015. Bacterial extracellular polysaccharides in biofilm formation and function. *Microbiology Spectrum*, 3(3).

Liu, H., Hu, Z., Li, M., Yang, Y., Lu, S. and Rao, X., 2023. Therapeutic potential of bacteriophage endolysins for infections caused by gram-positive bacteria. *Journal of Biomedical Science*, 30(29).

Liu, H., Kheirvari, M. and Tumban, E., 2023. Potential applications of thermophilic bacteriophages in one health. *International Journal of Molecular Sciences*, 24(9), p.8222.

Liu, S., Lu, H., Zhang, S., Shi, Y. and Chen, Q., 2022. Phages against Pathogenic Bacterial Biofilms and Biofilm-Based Infections: A Review. *Pharmaceutics*, 14(2), p.427.

Lopez-Miranda, J.L., Molina, G.A., González-Reyna, M.A., España-Sánchez, B.L., Esparza, R., Silva, R. and Estévez, M., 2023. Antibacterial and anti-inflammatory properties of ZnO nanoparticles synthesized by a green method using sargassum extracts. *International Journal of Molecular Sciences*, 24(2), p.1474.

Luo, Z., Yue, S., Chen, T., She, P., Wu, Y. and Wu, Y., 2020. Reduced growth of *Staphylococcus aureus* under high glucose conditions is associated with decreased pentaglycine expression. *Frontiers in Microbiology*, *11*, p.537290.

Lu, Y., Wang, Y., Wang, J., Zhao, Y., Zhong, Q., Li, G., Fu, Z. and Lu, S., 2021. Phage endolysin LysP108 showed promising antibacterial potential against methicillin-resistant *Staphylococcus aureus. Frontiers in Cellular and Infection Microbiology*, 11(668430).

Male, D., Peebles, R.S.J. and Male, V., 2020. *Immunology*. 9th ed. Poland: Elsevier.

Malik, M.A., Wani, M.Y. and Hashmi, A.A., 2020. Combination therapy: Current status and future perspectives. In: M.Y. Wani and A. Ahmad, eds. 2020. *Combination Therapy Against Multidrug Resistance*. Academic Press. pp.1-38.

Marano, R.J., Wallace, H.J., Wijeratne, D., Fear, M.W., Wong, H.S. and O'Handley, R., 2015. Secreted biofilm factors adversely affect cellular wound healing processes in vitro. *Scientific Reports*, 5(1).

Matilla-Cuenca, L., Taglialegna, A., Gil, C., Toledo-Arana, A., Lasa, I. and Valle, J., 2022. Bacterial biofilm functionalization through Bap amyloid engineering. *npj Biofilms and Microbiomes*, 8(1), p.62.

Mendhe, S., Badge, A., Ugemuge, S. and Chandi, D., 2023. Impact of biofilms on chronic infections and medical challenges. *Cureus*, 15(11), p.e48204.

Miao, J., Lin, S., Soteyome, T., Peters, B., Li, Y., Chen, H., Su, J., Li, L., Li, B., Xu, Z., Shirtliff, M.E. and Harro, J.M., 2019. Biofilm formation of *Staphylococcus aureus* under food heat processing conditions: first report on CML production within biofilm. *Scientific Reports*, 9(1), p.1312.

Mirzaei, R., Mohammadzadeh, R., Alikhani, M.Y., Shokri Moghadam, M., Karampoor, S., Kazemi, S., Barfipoursalar, A. and Yousefimashouf, R., 2020. The biofilm-associated bacterial infections unrelated to indwelling devices. *IUBMB Life*, 72(7), pp.1271-1285.

Mitchell, A.M. and Silhavy, T.J., 2019. Envelope stress responses: balancing damage repair and toxicity. *Nature Reviews Microbiology*, 17(7), pp.417–428.

Mlynarczyk-Bonikowska, B., Kowalewski, C., Krolak-Ulinska, A. and Marusza, W., 2022. Molecular mechanisms of drug resistance in *Staphylococcus aureus*. *International Journal of Molecular Science*, 23(15), p.8088.

Mishra, R., Panda, A.K., De Mandal, S., Shakeel, M., Bisht, S.S. and Khan, J., 2020. Natural anti-biofilm agents: strategies to control biofilm-forming pathogens. *Frontiers in Microbiology*, 11(566325).

Muhammad, M.H., Idris, A.L., Fan, X., Guo, Y., Yu, Y., Jin, X., Qiu, J., Guan, X. and Huang, T., 2020. Beyond risk: bacterial biofilms and their regulating approaches. *Frontiers in Microbiology*, 11(928), pp.1-20.

Murray, C.J., 2022. Global burden of bacterial antimicrobial resistance in 2019: a systematic analysis. *The Lancet*, 399(10325), pp.629–655.

Murray, E., Draper, L.A., Ross, R.P. and Hill, C., 2021. The advantages and challenges of using endolysins in a clinical setting. *Viruses*, 13(4), p.680.

Ng, Q.X., Ong, N.Y., Lee, D.Y.X., Yau, C.E., Lim, Y.L., Kwa, A.L. and Tan, B.H., 2023. Trends in *Pseudomonas aeruginosa* (*P. aeruginosa*) bacteremia during the COVID-19 pandemic: a systematic review. *Antibiotics*, 12(2), p.49.

Nguyen, N.T., Grelling, N., Wetteland, C.L., Rosario, R. and Liu, H., 2018. Antimicrobial activities and mechanisms of magnesium oxide nanoparticles (nMgO) against pathogenic bacteria, yeasts, and biofilms. *Scientific Reports*, 8(1), p.16260.

Ning, H., Lin, H., Wang, J., He, X., Lv, X. and Ju, L., 2021. Characterizations of the endolysin Lys84 and its domains from phage qdsa002 with high activities against *Staphylococcus aureus* and its biofilms. *Enzyme and Microbial Technology*, 148, p.109809.

Olsen, N.M.C., Thiran, E., Halser, T., Vanzieleghem, T., Belibasakis, G.N., Mahillon, J., Loessner, M.J. and Schmelcher, M., 2018. Synergistic removal of static and dynamic *Staphylococcus aureus* biofilms by combined treatment with a bacteriophage endolysin and a polysaccharide depolymerase. *Viruses*, 10(8), p.438.

Pachori, P., Gothalwal, R. and Gandhi, P., 2019. Emergence of antibiotic resistance *Pseudomonas aeruginosa* in intensive care unit; a critical review. *Genes & Diseases*, 6(2), pp.109–119.

Park, D.W. and Park, J.H., 2020. Characterization of endolysin LysECP26 derived from rV5-like Phage vB_EcoM-ECP26 for inactivation of *Escherichia coli* O157:H7. *Journal of Microbiology and Biotechnology*, 30(10), pp.1552–1558.

Parrino, B., Carbone, D., Cascioferro, S., Pecoraro, C., Giovannetti, E., Deng, D., Di Sarno, V., Musella, S., Auriemma, G., Cusimano, M.G., Schillaci, D., Cirrincione, G. and Diana, P., 2021. 1,2,4-oxadiazole topsentin analogs as staphylococcal biofilm inhibitors targeting the bacterial transpeptidase sortase A. *European Journal of Medicinal Chemistry*, 209, p.112892.

Patangia, D.V., Anthony Ryan, C., Dempsey, E., Paul Ross, R. and Stanton, C., 2022. Impact of antibiotics on the human microbiome and consequences for host health. *MicrobiologyOpen*, 11(1), p.e1260.

Pennone, V., Sanz-Gaitero, M., O'Connor, P., Coffey, A., Jordan, K., van Raaij, M.J. and McAuliffe, O., 2019. Inhibition of *L. monocytogenes* biofilm formation by the amidase domain of the phage vB_LmoS_293 endolysin. *Viruses*, 11(8), p.722.

Perry, E.K. and Tan, M.W., 2023. Bacterial biofilms in the human body: prevalence and impacts on health and disease. *Frontiers in Cellular and Infection Microbiology*, 13, pp.1-24.

Phang, Z., Raudonis, R., Glick, B.R., Lin, T.J. and Cheng, Z., 2019. Antibiotic resistance in *Pseudomonas aeruginosa*: mechanisms and alternative therapeutic strategies. *Biotechnology Advances*, 37(1), pp.177-192.

Phukan, C., Lahkar, M., Ranotkar, S. and Saikia, K.K., 2016. Emergence of *vanA* gene among vancomycin-resistant enterococci in a tertiary care hospital of North – East India. *The Indian Journal of Medical Research*, 143(3), pp.357-361.

Pinto, R.M., Soares, F.A., Reis, S., Nunes, C., Van Dijck, P., 2020. Innovative strategies toward the disassembly of the EPS matrix in bacterial biofilms. *Frontiers in Microbiology*, 11, p.952.

Pletzer, D., Mansour, S.C. and Hancock, R.E.W., 2018. Synergy between conventional antibiotics and anti-biofilm peptides in a murine, sub-cutaneous abscess model caused by recalcitrant ESKAPE pathogens. *PLoS Pathogens*, 14(6), p.e1007084.

Pommerville, J.C., 2021. *Fundamentals of microbiology*. 12th ed. Burlington: Jones & Bartlett Learning.

Preda, V.G. and Săndulescu, O., 2019. Communication is the key: biofilms, quorum sensing, formation and prevention. *Discoveries*, 7(3), p.e100.

Rahman, M.U., Wang, W., Sun, Q., Shah, J.A., Li, C., Sun, Y., Li, Y., Zhang, B., Chen, W. and Wang, S., 2021. Endolysin, a promising solution against antimicrobial resistance. *Antibiotics*, 10(11), p.1277.

Raoofi, S., Pashazadeh Kan, F., Rafiei, S., Hosseinipalangi, Z., Noorani Mejareh, Z., Khani, S., Abdollahi, B., Seyghalani Talab, F., Sanaei, M., Zarabi, F., Dolati, Y., Ahmadi, N., Raoofi, N., Sarhadi, Y., Masoumi, M., Sadat Hosseini, B., Vali, N., Gholamali, N., Asadi, S., Ahmadi, S., Ahmadi, B., Beiramy Chomalu, Z., Asadollahi, E., Rajabi, M., Gharagozloo, D., Nejatifar, Z., Soheylirad, R., Jalali, S., Aghajani, F., Navidriahy, M., Deylami, S., Nasiri, M., Zareei, M., Golmohammadi, Z., Shabani, H., Torabi, F., Shabaninejad, H., Nemati, A., Amerzadeh, M., Aryankhesal, A. and Ghashghaee, A., 2023. Global prevalence of nosocomial infection: a systematic review and meta-analysis. *PloS One*, 18(1), p.e0274248.

Rather, M.A., Gupta, K. and Mandal, M., 2021. Microbial biofilm: formation, architecture, antibiotic resistance, and control strategies. *Brazilian Journal of Microbiology*, 52(4), pp.1701-1718.

Reddersen, K., Güllmar, A., Tonndorf-Martini, S., Sigusch, B.W., Ewald, A., Dauben, T.J., Martin, K. and Wiegand, C., 2021. Critical parameters in cultivation of experimental biofilms using the example of Pseudomonas fluorescens. *Journal of Materials Science: Materials in Medicine*, 32(9), p.96.

Reygaert, W.C., 2018. An overview of the antimicrobial resistance mechanisms of bacteria. *AIMS Microbiology*, 4(3), pp.482-501.

Riedel, S., Hobden, J.A., Miller, S., Morse, S.A., Mietzner, T.A., Detrick, B., Mitchell, T.G., Sakanari, J.A., Hotez, P. and Mejia, R., 2019. *Jawetz, Melnick & Adelberg's medical microbiology*. 28th ed. New York: McGraw Hill Education.

Ríos, P., Rocha, C., Castro, W., Vidal, M., Canal, E., Bernal, M., Reynolds, N.D., Tilley, D.H., Jr. and Simons, M.P., 2018. Extensively drug-resistant (XDR) *Pseudomonas aeruginosa* identified in Lima, Peru co-expressing a VIM-2 metallo-β-lactamase, OXA-1 β-lactamase and GES-1 extended-spectrum β-lactamase. *Journal of Medical Microbiology Case Reports*, 5(7), p.e005154.

Roberts, R., 2016. *Biofilm protocol optimization for Pseudomonas aeruginosa*. [online] Available at: <https://imquestbio.com/wp-content/uploads/2016/09/Biofilm-Formation-Pseudomonas.pdf > [Accessed 22 March 2024].

Rohde, M., 2019. The gram-positive bacterial cell wall. *Microbiology Spectrum*, 7(3).

Roy, R., Tiwari, M., Donelli, G. and Tiwari, V., 2018. Strategies for combating bacterial biofilms: a focus on anti-biofilm agents and their mechanisms of action. *Virulence*, 9(1), pp.522-554.

Ryan, K.J. ed., 2022. *Sherris & Ryan's medical microbiology*. 8th ed. New York: McGraw Hill Education.

Salgar-Chaparro, S.J., Lepkova., K., Pojtanabuntoeng, T., Darwin, A. And Machuca, L.L., 2020. Nutrient level determines biofilm characteristics and subsequent impact on microbial corrosion and biocide effectiveness. *Applied and Environmental Microbiology*, 86(7), p.e02885-19.

Santajit, S. and Indrawattana, N., 2016. Mechanisms of antimicrobial resistance in eskape pathogens. *BioMed Research International*, 2016(2475067), pp.1–8.

Sanz-Gaitero, M., Keary, R., Garcia-Doval, C., Coffey, A. and Van Raaij, M.J., 2014. Crystal structure of the lytic CHAP(K) domain of the endolysin LysK from *Staphylococcus aureus* bacteriophage K. *Virology Journal*, 11, p.133.

Sar, T. and Akbar, M.Y., 2019. Glucose effect on biofilm formation of *S. aureus* strains. *Eurasian Journal of Biological and Chemical Sciences*, 2(2), pp.52-55.

Sato, Y., Ubagai, T., Tansho-Nagakawa, S., Yoshino, Y. and Ono, Y., 2021. Effects of colistin and tigecycline on multidrug-resistant *Acinetobacter baumannii* biofilms: advantages and disadvantages of their combination. *Scientific Reports*, 11(1), p.11700.

Schmelcher, M. and Loessner, M.J., 2021. Bacteriophage endolysins — extending their application to tissues and the bloodstream. *Current Opinion in Biotechnology*, 68, pp.51–59.

Schulze, A., Mitterer, F., Pombo, J.P. and Schild, S., 2021. Biofilms by bacterial human pathogens: clinical relevance – development, composition and regulation – therapeutic strategies. *Microbial Cell*, 8(2), pp.28-56.

Sharma, D., Misba, L. and Khan, A.U., 2019. Antibiotics versus biofilm: an emerging battleground in microbial communities. *Antimicrobial Resistance & Infection Control*, 8(76).

Sharma, S., Mohler, J., Mahajan, S.D., Schwartz, S.A., Bruggemann, L. and Aalinkeel, R., 2023. Microbial biofilm: a review on formation, infection, antibiotic resistance, control measures, and innovative treatment. *Microorganisms*, 11(6), p.1614.

She, P., Wang, Y., Liu, Y., Tan, F., Chen, L., Luo, Z. and Wu, Y., 2019. Effects of exogenous glucose on *Pseudomonas aeruginosa* biofilm formation and antibiotic resistance. *Microbiology Open*, 8(12), p.e933.

Shineh, G., Mobaraki, M., Perves Bappy, M.J. and Mills, D.K., 2023. Biofilm formation, and related impacts on healthcare, food processing and packaging, industrial manufacturing, marine industries, and sanitation–a review. *Applied Microbiology*, 3(3), pp.629–665.

Singh, A.K., Prakash, P., Achra, A., Singh, G. P., Das, A. and Singh, R.K., 2017. Standardization and classification of in vitro biofilm formation by clinical isolates of *Staphylococcus aureus*. *Journal of Global Infectious Diseases*, 9(3), pp.93-101.

Singh, S., Datta, S., Narayanan, K.B. and Rajnish, K.N., 2021. Bacterial exo-polysaccharides in biofilms: role in antimicrobial resistance and treatments. *Journal of Genetic Engineering and Biotechnology*, 19(1), p.140.

Son, B., Kong, M., Cha, Y., Bai, J. and Ryu, S., 2020. Simultaneous control of *Staphylococcus aureus* and *Bacillus cereus* using a hybrid endolysin LysB4EAD-LysSA11. *Antibiotics*, 9(12), p.906.

Soontarach, R., Srimanote, P., Voravuthikunchai, S.P. and Chusri, S., 2024. Antibacterial and anti-biofilm efficacy of endolysin LysAB1245 against a panel of important pathogens. *Pharmaceuticals*, 17(2), p.155.

Su, Y., Yrastorza, J.T., Matis, M., Cusick, J., Zhao, S., Wang, G. and Xie, J., 2022. Biofilms: formation, research models, potential targets, and methods for prevention and treatment. *Advanced Science*, 9(29), p.e2203291.

Swidan, N.S., Hashem, Y.A., Elkhatib, W.F. and Yassien, M.A., 2022. Antibiofilm activity of green synthesized silver nanoparticles against biofilm associated enterococcal urinary pathogens. *Scientific Reports*, 12(3869).

Tan, S.Y., Khan, R.A., Khalid, K.E., Chong, C.W. and Bakhtiar, A., 2022. Correlation between antibiotic consumption and the occurrence of multidrug-resistant organisms in a Malaysian tertiary hospital: a 3-year observational study. *Scientific Reports*, 12(3106).

Tankeshwar, A., 2013. *Lipopolysaccharide (LPS) layer*. [online] Available at: <https://microbeonline.com/lipopolysaccharide-lps-of-gram-negative-bacteria-characteristics-and-functions/> [Accessed 16 February 2024].

Taylor, T.A. and Unakal, C.G., 2023. *Staphylococcus aureus infection*. [online] Available at: <https://www.ncbi.nlm.nih.gov/books/NBK441868/> [Accessed 21 January 2024].

Thieme, L., Hartung, A., Tramm, K., Klinger-Strobel, M., Jandt, K.D., Makarewicz, O. and Pletz, M.W., 2019. MBEC versus MBIC: the lack of differentiation between biofilm reducing and inhibitory effects as a current problem in biofilm methodology. *Biological Procedures Online*, 21(18).

Umemura, T., Kato, H., Hagihara, M., Hirai, J., Yamagishi, Y. and Mikamo, H., 2022. Efficacy of combination therapies for the treatment of multi-drug resistant gram-negative bacterial infections based on meta-analyses. *Antibiotics*, 11(4), p.524.

Vandana and Das, S., 2022. Genetic regulation, biosynthesis and applications of extracellular polysaccharides of the biofilm matrix of bacteria. *Carbohydrate Polymers*, 291, p.119536.

Van Der Schoor, A.S., Voor In 't Holt, A.F., Zandijk, W.H.A., Bruno, M.J., Gommers, D., Van Der Akker, J.P.C., Hendriks, J.M., Severin, J.A., Klaassen, C.H.W. and Vos, M.C., 2023. Dynamic of *Staphylococcus aureus* in patients and the hospital environment in a tertiary care hospital in the Netherlands. *Antimicrobial Resistance and Infection Control*, 12(148).

Vestby, L.K., Grønseth, T., Simm, R. and Nesse, L.L., 2020. Bacterial biofilm and its role in the pathogenesis of disease. *Antibiotics*, 9(2), p.59.

Villines, Z., 2023. *What are some of the effects of overusing antibiotics?* [online] Available at: <https://www.medicalnewstoday.com/articles/effects-of-overusing-antibiotics> [Accessed 13 January 2024].

Vyas, V. and Goyal, A., 2022. *Acute pulmonary embolism*. [online] Available at: <https://www.ncbi.nlm.nih.gov/books/NBK560551/> [Accessed 18 February 2024].

Wang, Q., Vachon, J., Prasad, B., Pybus, C.A., Lapin, N., Chopra, R. and Greenberg, D.E., 2021. Alternating magnetic fields and antibiotics eradicate biofilm on metal in a synergistic fashion. *NPJ Biofilms and Microbiomes*, 7(1), p.68.

Wang, J., Liang, S., Lu, X., Xu, Q., Zhu, Y., Yu, S., Zhang, W., Liu, S. and X, F., 2023. Bacteriophage endolysin Ply113 as a potent antibacterial agent against polymicrobial biofilms formed by enterococci and *Staphylococcus aureus*. *Frontiers in Microbiology*, 14.

Willey, J.M., Sandman, K. and Wood, D., 2020. *Prescott's microbiology*. 11th ed. New York: Mcgraw-Hill.

Wilson, M.G. and Pandey, S., 2023. *Pseudomonas aeruginosa*. [online] Available at: <https://www.ncbi.nlm.nih.gov/books/NBK557831/> [Accessed 11 January 2024].

Wolfmeier, H., Pletzer, D., Mansour, S.C. and Hancock, R.E.W., 2018. New perspectives in biofilm eradication. *ACS Infectious Diseases*, 4(2), p.93.

World Health Organization, 2023. *Antimicrobial resistance*. [online] Available at: <https://www.who.int/news-room/fact-sheets/detail/antimicrobial-resistance> [Accessed 1 January 2023].

Xu, D., Zhao, S., Dou, J., Xu, X., Zhi, Y. and Wen, L., 2021. Engineered endolysin-based "artilysins" for controlling the gram-negative pathogen *Helicobacter pylori*. *AMB Express*, 11(1), p.63.

Yang, D., Chen, Y., Sun, E., Hua, L., Peng, Z. and Wu, B., 2020. Characterization of a lytic bacteriophage vB_EfaS_PHB08 harboring endolysin Lys08 against *Enterococcus faecalis* biofilms. *Microorganisms*, *8*(9), p.1332.

Yang, S., Li, X., Cang, W., Mu, D., Ji, S., An, Y., Wu, R. and Wu, J., 2023. Biofilm tolerance, resistance and infections increasing threat of public health. *Microbial Cell*, 10(11), pp.233–247.

Yasir, M., Willcox, M.D.P. and Dutta, D., 2018. Action of antimicrobial peptides against bacterial biofilms. *Materials*, 11(12), p.2468.

Yi, L., Li, X., Luo, L., Lu, Y., Yan, H., Qiao, Z. and Lü, X., 2018. A novel bacteriocin BMP11 and its antibacterial mechanism on cell envelope of *Listeria monocytogenes* and *Cronobacter sakazakii*. *Food Control*, 91, pp.160-169.

Yuen, H.L., Chan, S.Y., Ding, Y.E., Lim, S., Tan, G.C. and Kho, C.L., 2023. Development of a novel antibacterial peptide, PAM-5, via combination of phage display selection and computer-assisted modification. *Biomolecules*, 13, p.466.

Zhang, Y., Huang, H.H., Duc, H.M., Masuda, Y., Honjoh, K.I. and Miyamoto, T., 2021. Endolysin LysSTG2: characterization and application to control *Salmonella Typhimurium* biofilm alone and in combination with slightly acidic hypochlorous water. *Food Microbiology*, 98, p.103791.

Zhang, Y., Huang, H.H., Duc, H.M., Masuda, Y., Honjoh, K.I. and Miyamoto, T., 2022. Application of endolysin LysSTG2 as a potential biocontrol agent against planktonic and biofilm cells of Pseudomonas on various food and food contact surfaces. *Food Control*, 131, p.108460.

Zhao, A., Sun, J. and Liu, Y., 2023. Understanding bacterial biofilms: from definition to treatment strategies. *Frontiers in Cellular and Infection Microbiology*, 13, pp.1-23.

Appendix A

Table 1: List of chemicals and reagents that had been utilized throughout the study.

Chemicals/reagents	Manufacturer
Acrylamide	Bio Basic Inc., Canada
Ammonium persulfate	Merck KGaA, Germany
Beta-mercaptoethanol	Bio Basic Inc., Canada
Bis acrylamide	EMD Chemicals Inc., United State
Bovine serum albumin (BSA)	VWR International Ltd., United Kingdom
Bradford reagent	Chemiz, Malaysia
Bromophenol blue	GE Healthcare Bio-Science AB, Sweden
Coomassie blue	Merck KGaA, Germany
Crystal violet	Chemical Solutions Sdn. Bhd., Malaysia
D-glucose	Bio Basic Inc., Canada
Di-sodium hydrogen phosphate	Classic Chemicals, Malaysia
Ethanol	Classic Chemicals, Malaysia
Ethylenediaminetetraacetic acid (EDTA)	Fisher Scientific International Inc., United State
Glacial acetic acid	QRëC, Malaysia
Glycerol (99.5%)	QRëC, Malaysia
Glycine	R&M Marketing, United Kingdom
Hydrochloric acid (37%)	Fisher Scientific International Inc., United State
Imidazole	Sisco Research Laboratories Pvt. Ltd.
Isopropanol	Merck KGaA, Germany
Isopropyl-B-D-1-thiogalactopyranoside (IPTG)	Sisco Research Laboratories Pvt. Ltd.
Kanamycin	Bio Basic Inc., Canada
LB agar (Lennox)	Laboratorios Conda S.A., Spain
LB broth (Lennox)	Laboratorios Conda S.A., Spain
Lysozyme	Merck KGaA, Germany
Methanol	Chemiz, Malaysia
N-butanol	Merck KGaA, Germany
Nickel (Ni) resin	BioLabs Inc., United States
Nickel(II) sulfate hexahydrate	Merck KGaA, Germany
Ortho-phosphoric acid 85%	RCI Labscan Limited, Thailand

Table 1: List of chemicals and reagents that had been utilized throughout the study (continue).

Sodium chloride	Merck KGaA, Germany
Sodium dihydrogen phosphate monohydrate	Merck KGaA, Germany
Sodium dodecyl sulfate (SDS)	Bio Basic Inc., Canada
Sodium hydroxide	R&M Marketing, United Kingdom
TEMED	EMD Millipore Corporation, United States
Tris	Bio Basic Inc., Canada
Tris hydrochloride	Bio Basic Inc., Canada
Tryptic soy broth (Lennox)	Merck KGaA, Germany
Whole blue range pre-stained protein ladder	Vivantis Technologies Sdn. Bhd., Malaysia

Table 2: List of equipment and laboratory wares that had been utilized throughout the study.

Equipment/Laboratory Wares	Manufacturer
96-well plates (flat bottom)	Wuxi Nest Biotechnology Co. Ltd., China
Analytical balance	KERN & SOHN, Germany
Autoclave machine	Hiramaya, Japan
Beakers	DURAN, Germany
Biosafety cabinet level 2	Telstar, Philippines
Centrifuge tubes (15 mL and 50 mL)	Wuxi Nest Biotechnology Co. Ltd., China
Drying incubator	Memmert, Germany
Flexi incubator	Memmert, Germany
Freezer (-20 °C)	Eppndorf, United Kingdom
Gel imager	Bio rad
Incubator	Memmert, Germany
Laminar hood	ESCO, Singapore
Magnetic stirrer	Stuart, United Kingdom
Measuring cylinders	PLT Scientific Sdn Bhd., Malaysia
Media bottles	DWK Life Sciences GmbH, Germany
Microcentrifuge	Beckman Coulter, Germany
Microcentrifuge tubes (0.5 mL and 1.5 mL)	Biosharp Beijing Labgic Technology Co., Ltd., China
Micropipette tips (10 µL, 200 µL, 1000 µL)	Wuxi Nest Biotechnology Co. Ltd., China
Microplate reader	BMG Labtech FLUOstar Omega, Australia
Petri dishes	Brandon, Malaysia
pH meter	Eutech Instruments, Singapore
Refrigerated benchtop centrifuge	Sigma Laborzentrifugen GmbH, Germany
SDS-PAGE set	Bio-rad Laboratories Inc., Malaysia
See saw rocker	Stuart, United Kingdom
Shaking incubator	Yihder Co. Ltd., Taiwan
Shaking incubator with cooling	Infors HT, Switzerland
Snakeskin pleated dialysis tubing	Thermo Scientific, USA
Spectrophotometer	DLAB, China
Syringe (5 mL/cc)	Terumo Corporation, Phillipines
Syringe filter (0.22 um, 0.45 um)	Bioflow Lifescience Sdn Bhd., Malaysia
Vortex	Gemmy, Taiwan
Water bath	Memmert, Germany